

- a. For each of the values  $M = 20, 50, 100, 200$ , solve Hallén's equation for a delta-gap input with voltage  $V_0 = 1$  volt using both the exact and the approximate kernels. Plot the real and imaginary parts of the current  $I_m = I(z_m)$  versus  $z_m$  over the right half of the antenna, that is,  $0 \leq z_m \leq h$ , where  $h = l/2$ .
- b. Fit to the computed current samples  $I_m$  of the exact kernel to King's three-term approximation. Then, place the fitted points on the same graphs as in part (a). Discuss how well or not the three-term approximation fits the exact-kernel and the approximate-kernel current.  
Repeat by using a two-term approximation. Discuss how well or not the two-term approximation fits the exact-kernel and the approximate-kernel current.
- c. To illustrate the logarithmic singularity near  $z = 0$ , evaluate the limiting expression at the points  $z_m$ ,  $m = 1, 2, \dots, M$ , for  $M = 200$  (the point  $z_0 = 0$  is to be skipped):

$$I_{\log}(z_m) = -j \frac{4kaV_0}{\eta} \ln(k|z_m|) + \text{const.}$$

Adjust the constant so that this expression agrees with the exact-kernel current at the point  $z_1$ , that is,  $I_{\log}(z_1) = I_1$ . Then, plot the imaginary parts of  $I_m$  and  $I_{\log}(z_m)$  versus  $z_m$ .

- d. Repeat parts (a-c) for the antenna radius  $a = 0.001$  and then for  $a = 0.008$ . Discuss the effect of changing the radius on the quality of the solution, both for the exact and the approximate kernel cases.
- e. Repeat parts (a-d) for the antenna length  $l = 1.0\lambda$ . Comment on the success of the exact versus approximate kernel calculations versus the parameters  $l, a, M$ .
- f. For each value of  $M$  and current solution  $I_m$ ,  $-M \leq m \leq M$ , the input impedance of the antenna can be calculated from the center sample  $I_0$ , that is,  $Z_0 = V_0/I_0$ . Similarly, the input admittance is:

$$Y_0 = \frac{1}{Z_0} = \frac{I_0}{V_0} = G_0 + jB_0$$

where  $G_0, B_0$  are its real and imaginary parts, that is, the input conductance and susceptance.

For each of the values  $M = 1, 2, \dots, 100$ , calculate the corresponding conductance and susceptance,  $G_0(M), B_0(M)$ , using the exact and the approximate kernels and plot them versus  $M$ . Use the length and radius  $l = 0.5\lambda$  and  $a = 0.005\lambda$ .

This is a time-consuming question. It requires that you solve the Hallén equation for each value of  $M$  for the exact and approximate kernels and pick the center value  $I_0$ . Discuss the convergence properties of the exact versus the approximate kernel calculation.

### 25.1 Near Fields of Linear Antennas

In calculating mutual coupling effects between closely-spaced linear antennas, we need to know the fields produced by an antenna at near distances. The fields generated by a thin wire antenna with current  $I(z)$  were worked out in Sec. 15.4.

We summarize these results here. All field components can be obtained from the knowledge of the  $z$ -component of the magnetic vector potential  $A_z(z, \rho)$ :

$$A_z(z, \rho) = \frac{\mu}{4\pi} \int_{-h}^h I(z') \frac{e^{-jkR}}{R} dz', \quad R = \sqrt{\rho^2 + (z - z')^2} \quad (25.1.1)$$

where  $h$  is the half-length of the antenna,  $h = l/2$ , and the geometry is shown in Fig. 25.1.1. We have used the approximate thin-wire kernel because it differs little from the exact kernel for distances  $\rho > a$  (typically, when  $\rho \gtrsim 5a$ .)

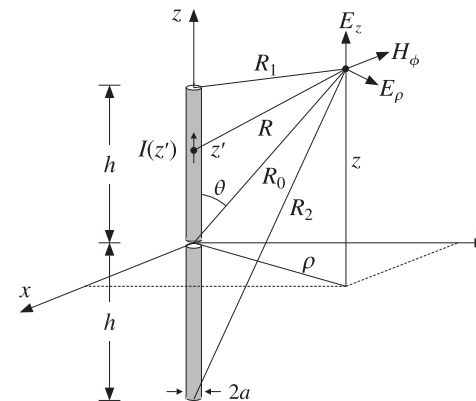


Fig. 25.1.1 Fields of a thin wire antenna.

Then, the non-zero field components  $E_z, E_\rho, H_\phi$  can be constructed from the two alternative sets of formulas:

$$\left[ \begin{array}{l} j\omega\mu\epsilon E_z = \partial_z^2 A_z + k^2 A_z \\ j\omega\mu\epsilon E_\rho = \partial_\rho \partial_z A_z \\ \mu H_\phi = -\partial_\rho A_z \end{array} \right], \quad \left[ \begin{array}{l} j\omega\mu\epsilon E_z = \partial_z^2 A_z + k^2 A_z \\ \partial_\rho(\rho H_\phi) = j\omega\epsilon \rho E_z \\ j\omega\epsilon E_\rho = -\partial_z H_\phi \end{array} \right] \quad (25.1.2)$$

As a first approximation, we will assume that the current  $I(z)$  is sinusoidal. This is justified only when the antenna length is near half a wavelength  $\lambda/2$ . Most coupled antenna arrays that are used in practice, such as Yagi-Uda, satisfy this condition.

We note also that the near fields resulting from the sinusoidal current assumption do not satisfy the correct boundary conditions on the surface of the antenna, that is the condition  $E_z(z, \rho) = 0$  at  $z \neq 0$  and  $\rho = a$ . In Sec. 25.2, we consider an improved approximation of the near fields that addresses these issues. Thus for now, we will assume that:

$$I(z) = I_0 \frac{\sin(k(h - |z|))}{\sin kh} = I_m \sin(k(h - |z|)) \quad (25.1.3)$$

where we distinguish between the current  $I_0$  at  $z = 0$  and the maximum current  $I_m = I_0 / \sin kh$ . For half-wavelength antennas, we have  $kh = \pi/2$ ,  $I_0 = I_m$ , and the current becomes  $I(z) = I_0 \cos kz$ .

In principle, one could insert Eq. (25.1.3) into (25.1.1) and perform the required integrations to get  $A_z$ . However, for the purpose of determining the fields, this is not necessary. Combining (25.1.1) and (25.1.2), we obtain:

$$j\omega\mu\epsilon E_z(z, \rho) = \partial_z^2 A_z + k^2 A_z = \frac{\mu}{4\pi} \int_{-h}^h I(z') (\partial_z^2 + k^2) G(z - z', \rho) dz' \quad (25.1.4)$$

where we denoted  $G(z - z', \rho) = e^{-jkR}/R$  and replaced  $\partial_z^2$  by  $\partial_z'^2$ . Next, we use the differential identity:

$$I(\partial_z'^2 + k^2)G - G(\partial_z'^2 + k^2)I = \partial_z' [I\partial_z'G - G\partial_z'I] \quad (25.1.5)$$

Because of the assumed form (25.1.3),  $I(z')$  satisfies the Helmholtz equation,  $(\partial_z'^2 + k^2)I(z') = 0$ , and therefore, the integrand of (25.1.4) becomes a complete derivative:

$$I(z') (\partial_z'^2 + k^2)G(z - z', \rho) = \partial_z' [I(z')\partial_z'G(z - z', \rho) - G(z - z', \rho)\partial_z'I(z')] \quad (25.1.6)$$

Integrating the first term, we obtain:

$$\int_{-h}^h \partial_z' [I(z')\partial_z'G(z - z', \rho)] dz' = I(h)\partial_z'G(z - h, \rho) - I(-h)\partial_z'G(z + h, \rho) = 0$$

where we used the end-conditions  $I(h) = I(-h) = 0$ . The second term in (25.1.6) is a little trickier because  $\partial_z'I(z')$  is discontinuous at  $z = 0$ . Splitting the integration range, we obtain:

$$\begin{aligned} \int_{-h}^h \partial_z' [G(z - z', \rho)\partial_z'I(z')] dz' &= \left( \int_{-h}^0 + \int_0^h \right) \partial_z' [G(z - z', \rho)\partial_z'I(z')] dz' \\ &= [G(z, \rho)I'(0-) - G(z + h, \rho)I'(-h)] + [G(z - h, \rho)I'(h) - G(z, \rho)I'(0+)] \\ &= kI_m [2 \cos kh G(z, \rho) - G(z - h, \rho) - G(z + h, \rho)] \end{aligned}$$

where we used  $I'(0\pm) = \mp kI_m \cos kh$  and  $I'(\pm h) = \mp kI_m$ . Inserting this result into Eq. (25.1.4) and rearranging some constants, we find:

$$E_z(z, \rho) = -\frac{j\eta I_m}{4\pi} [G(z - h, \rho) + G(z + h, \rho) - 2 \cos kh G(z, \rho)] \quad (25.1.7)$$

The quantities  $G(z - h, \rho), G(z + h, \rho), G(z, \rho)$  can be written conveniently as follows:

$$\begin{aligned} G(z, \rho) &= \frac{e^{-jkR_0}}{R_0}, & R_0 &= \sqrt{\rho^2 + z^2} \\ G(z - h, \rho) &= \frac{e^{-jkR_1}}{R_1}, & R_1 &= \sqrt{\rho^2 + (z - h)^2} \\ G(z + h, \rho) &= \frac{e^{-jkR_2}}{R_2}, & R_2 &= \sqrt{\rho^2 + (z + h)^2} \end{aligned} \quad (25.1.8)$$

where  $R_0, R_1, R_2$  are recognized to be the distances from the center and the two ends of the antenna to the observation point, as shown in Fig. 25.1.1. Thus, we can write:

$$E_z(z, \rho) = -\frac{j\eta I_m}{4\pi} \left[ \frac{e^{-jkR_1}}{R_1} + \frac{e^{-jkR_2}}{R_2} - 2 \cos kh \frac{e^{-jkR_0}}{R_0} \right] \quad (25.1.9)$$

Next, we determine  $H_\phi$  from Ampère's law in (25.1.2) by noting that  $\rho E_z$  is a complete derivative with respect to  $\rho$ . Indeed, for any of the quantities  $R$ , we have:

$$\partial_\rho(e^{-jkR}) = -jk(\partial_\rho R)e^{-jkR} = -jk\rho \frac{e^{-jkR}}{R} \Rightarrow \frac{e^{-jkR}}{R} = -\frac{1}{jk\rho} \partial_\rho(e^{-jkR})$$

Applying this result to all three terms of Eq. (25.1.9), we have:

$$\rho E_z(z, \rho) = -\frac{j\eta I_m}{4\pi} \frac{1}{-jk} \partial_\rho [e^{-jkR_1} + e^{-jkR_2} - 2 \cos kh e^{-jkR_0}]$$

Inserting this into Ampère's law,  $\partial_\rho(\rho H_\phi) = j\omega\epsilon \rho E_z$ , and rearranging some constants, we find:

$$\partial_\rho(\rho H_\phi) = \frac{jI_m}{4\pi} \partial_\rho [e^{-jkR_1} + e^{-jkR_2} - 2 \cos kh e^{-jkR_0}]$$

which can be integrated trivially, giving:

$$H_\phi(z, \rho) = \frac{jI_m}{4\pi\rho} [e^{-jkR_1} + e^{-jkR_2} - 2 \cos kh e^{-jkR_0}] \quad (25.1.10)$$

A possible integration constant in  $\rho$  is dropped because the field must vanish when its source vanishes, that is, when  $I_m = 0$ . Finally, we obtain  $E_\rho$  from Faraday's law in (25.1.2). Noting the differentiation property:

$$\partial_z(e^{-jkR}) = -jk \frac{z}{R} e^{-jkR}, \quad R = \sqrt{\rho^2 + z^2}$$



it follows from Eq. (25.2.4) that,

$$4\pi j\omega\epsilon E_z(z, \rho) = \int_{-h}^h G(z-z', \rho) \left[ I''(z') + k^2 I(z') \right] dz' - \left[ G(z-z', \rho) I'(z') \right]_{-h}^{0-} - \left[ G(z-z', \rho) I'(z') \right]_{0+}^h$$

which gives,

$$4\pi j\omega\epsilon E_z(z, \rho) = \int_{-h}^h G(z-z', \rho) \left[ I''(z') + k^2 I(z') \right] dz' + 2I'(0+)G(z, \rho) - I'(h) \left[ G(z-h, \rho) + G(z+h, \rho) \right] \quad (25.2.5)$$

where we used  $I'(h) = -I'(-h)$ . Finally, we can write,

$$4\pi j\omega\epsilon E_z(z, \rho) = \int_{-h}^h \frac{e^{-jkR}}{R} \left[ I''(z') + k^2 I(z') \right] dz' + 2I'(0+) \frac{e^{-jkR_0}}{R_0} - I'(h) \left[ \frac{e^{-jkR_1}}{R_1} + \frac{e^{-jkR_2}}{R_2} \right] \quad (25.2.6)$$

The last three terms are the standard terms found in the previous section. The principal-value integral term represents the correction that must be added to enable the boundary conditions. The other field components can now be obtained from  $E_z$  using similar procedures as in the previous section. For  $H_\phi$ , we find:

$$-4\pi jk\rho H_\phi(z, \rho) = \int_{-h}^h e^{-jkR} \left[ I''(z') + k^2 I(z') \right] dz' + 2I'(0+)e^{-jkR_0} - I'(h) \left[ e^{-jkR_1} + e^{-jkR_2} \right] \quad (25.2.7)$$

which may also be written in the form:

$$-4\pi jk\rho H_\phi(z, \rho) = \int_{-h}^h I(z') (\partial_z^2 + k^2) e^{-jkR} dz' \quad (25.2.8)$$

obtained by reversing the above differential identity steps. Similarly, we have:

$$-4\pi j\omega\epsilon\rho E_\rho(z, \rho) = \int_{-h}^h \frac{z-z'}{R} e^{-jkR} \left[ I''(z') + k^2 I(z') \right] dz' + 2I'(0+) \frac{z}{R_0} e^{-jkR_0} - I'(h) \left[ \frac{z-h}{R_1} e^{-jkR_1} + \frac{z+h}{R_2} e^{-jkR_2} \right] \quad (25.2.9)$$

which may also be written as,

$$-4\pi j\omega\epsilon\rho E_\rho(z, \rho) = \int_{-h}^h I(z') (\partial_z^2 + k^2) \left( \frac{z-z'}{R} e^{-jkR} \right) dz' \quad (25.2.10)$$

Our procedure for obtaining improved near fields is to first get an improved solution for the current  $I(z)$  and then use it in Eq. (25.2.6) to calculate the field  $E_z(z, \rho)$ . We will use the three-term approximation for the current:

$$I(z) = A_1 [\sin(k|z|) - \sin(kh)] + A_2 [\cos(kz) - \cos(kh)] + A_3 \left[ \cos\left(\frac{kz}{2}\right) - \cos\left(\frac{kh}{2}\right) \right] \quad (25.2.11)$$

and fix the coefficients  $A_1, A_2, A_3$  by fitting this expression to a numerical solution as discussed in Sec. 24.6, and then, use Eq. (25.2.11) into (25.2.6) with the integral term evaluated numerically. Fig. 25.2.1 shows the results of such a calculation for a half-wave antenna  $l = 0.5\lambda$  with radius  $a = 0.005\lambda$ . Fig. 25.2.2 shows the results for a full-wave antenna  $l = 1.0\lambda$  with the same radius. The required quantities appearing in (25.2.6) are calculated as follows:

$$I''(z') + k^2 I(z') = -k^2 A_1 \sin kh - k^2 A_2 \cos kh - k^2 A_3 \left[ \cos\left(\frac{kh}{2}\right) - \frac{3}{4} \cos\left(\frac{kz'}{2}\right) \right]$$

$$I'(0+) = -I'(0-) = kA_1$$

$$I'(h) = -I'(-h) = kA_1 \cos kh - kA_2 \sin kh - \frac{1}{2} kA_3 \sin\left(\frac{kh}{2}\right)$$

The numerical solutions were obtained by solving the Hallén equation with point-matching, pulse basis functions, and the exact kernel using  $M = 100$  upper-half current samples  $I_n$ . These current samples were then used as in Eq. (24.6.15) to obtain the parameters  $A_1, A_2, A_3$ .

The upper-left graphs show the current  $I(z)$  of Eq. (25.2.11) together with the samples  $I_n$  to which it was fitted.

The upper-right graphs show the magnitude of  $E_z(z, \rho)$  as a function of  $\rho$  for  $z$  fixed at  $z = 0.2h$ . The behavior of  $E_z(z, \rho)$  is consistent initially with a logarithmic dependence on  $\rho$  as predicted by King and Wu [1730,1731] and discussed below, followed then by the expected  $1/\rho$  decrease arising from the last three standard terms of Eq. (25.2.6), which are represented by the dashed curves.

The left middle-row graphs display the logarithmic dependence more clearly by plotting the real and imaginary parts of  $E_z(z, \rho)$  versus  $\ln(\rho/a)$ , including the King-Wu approximation of Eq. (25.2.15).

The right middle-row graphs show the magnitude of the field  $E_z(z, a)$  at the surface of the antenna as a function of  $z$  over the interval  $0 \leq z \leq h$ . Except at the feed and end points, the field is effectively zero as required by the boundary conditions.

To observe the importance of the correction term, that is, the principal-value integral in Eq. (25.2.6), the third-row graphs display the real and imaginary parts of  $E_z(z, a)$  versus  $z$ . Plotted separately are also the correction and standard terms, which appear always to have opposite signs canceling each other so that the net field is zero.

The graphs for Fig. 25.2.1 were generated by the following MATLAB code (for Figure 25.2.2 simply set  $L=1$ ):

```
L = 0.5; h = L/2; a = 0.005; k = 2*pi; eta = 377;
M = 100; [In,zn] = hdelta(L,a,M,'e','p'); % Hallen solution
```

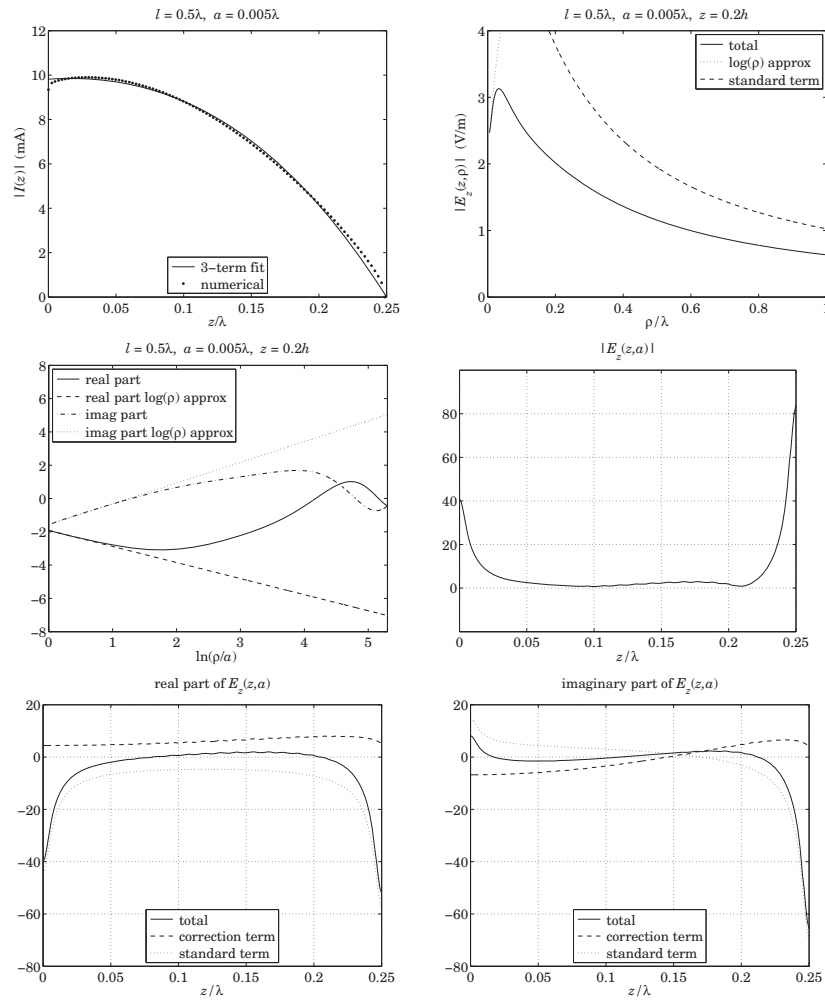


Fig. 25.2.1 Calculated near field  $E_z(z, \rho)$  for  $l = 0.5\lambda$ .

```
Inp = In(M+1:end); znp = zn(M+1:end); % keep upper-half only
z = 0:h/100:h;
A = kingfit(L,Inp,znp,3); I = kingeval(L,A,z); % 3-term fit
s = 1000; % scale in units of mA
plot(z,abs(I)*s,'-', znp,abs(Inp)*s,'.', 'markersize',11); % upper-left graph

I1h = k*(A(1)*cos(k*h) - A(2)*sin(k*h) - A(3)/2 * sin(k*h/2)); % I'(h)
I10 = A(1)*k; % I'(0+)
```

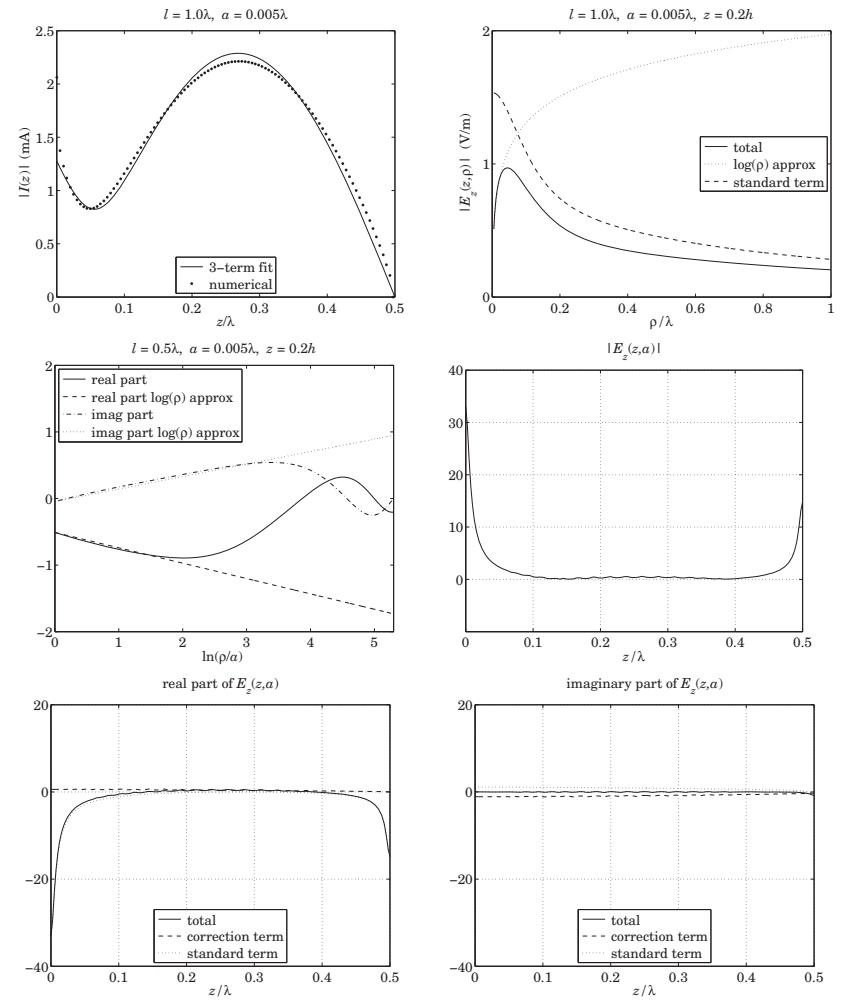


Fig. 25.2.2 Calculated near field  $E_z(z, \rho)$  for  $l = 1.0\lambda$ .

```
G = @(x,r) exp(-j*k*sqrt(x.^2 + r.^2))./sqrt(x.^2 + r.^2); % kernel function
Helm = @(z) -k^2*(A(1)*sin(k*h) + A(2)*cos(k*h) + A(3)*(cos(k*h/2)-3/4*cos(k*z/2)));
z = 0.2*h; r = linspace(a,200*a, 1001); logr = log(r/a);
S = -j*eta/4/pi/k; % scale factor, note omega*epsilon = k/eta

[wi,zi] = quadrs([-h,0,h],32); % quadrature weights and evaluation points
for i=1:length(r),
```

```

GHelm = G(z-zi,r(i)) .* Helm(zi);
E1(i) = (wi'*GHelm) * S; % correction term
E2(i) = (- I1h * (G(z-h,r(i)) + G(z+h,r(i))) + 2*I10 * G(z,r(i))) * S;
E(i) = E1(i) + E2(i);
end

Eapp = E(1) - Helm(z) * logr * 2*S; % King-Wu approximation adjusted by Ez(z,a)

figure; plot(r,abs(E), r,abs(Eapp),'-', r,abs(E2),'--'); % upper-right graph
figure; plot(logr,real(E), logr,real(Eapp),'-',...
            logr,imag(E),'-', logr,imag(Eapp),'-'); % middle-left graph

clear E E1 E2;
z = linspace(0,h,201); r = a;

for i=1:length(z),
    GHelm = G(z(i)-zi,r) .* Helm(zi);
    E1(i) = (wi'*GHelm) * S;
    E2(i) = (- I1h * (G(z(i)-h,r) + G(z(i)+h,r)) + 2*I10 * G(z(i),r)) * S;
    E(i) = E1(i) + E2(i);
end

figure; plot(z,abs(E),'-'); % middle-right graph
figure; plot(z,real(E), z,real(E1),'--', z,real(E2),'-'); % lower-left graph
figure; plot(z,imag(E), z,imag(E1),'--', z,imag(E2),'-'); % lower-right graph

```

Next, we discuss the King-Wu small- $\rho$  approximation [1730,1731]; see also McDonald [1785]. First, we note that the  $H_\phi$  and  $E_\rho$  components in Eqs. (25.2.8) and (25.2.10) were obtained by using Maxwell's equations (25.1.2), that is, Ampère's laws  $\partial_\rho(\rho H_\phi) = j\omega\epsilon\rho E_z$  and  $j\omega\epsilon E_\rho = -\partial_z H_\phi$ . We may also verify Faraday's law, which has only a  $\phi$  component in this case:

$$\partial_\rho E_z - \partial_z E_\rho = j\omega\mu H_\phi \quad (25.2.12)$$

Indeed, this can be derived from Eqs. (25.2.3), (25.2.8), and (25.2.10) by using the identity:

$$\rho \frac{\partial}{\partial \rho} \left( \frac{e^{-jkR}}{R} \right) + \frac{\partial}{\partial z} \left( \frac{z-z'}{R} e^{-jkR} \right) = -jke^{-jkR}$$

For a thin antenna, the small- $\rho$  dependence of  $H_\phi$  is obtained by taking the limit  $\rho \rightarrow 0$  in the right-hand side of Eq. (25.2.8). In this limit, we have  $e^{-jkR} = e^{-jk|z-z'|}$ , which is recognized as the Green's function of the one-dimensional Helmholtz equation discussed in Sec. 24.3 that satisfies  $(\partial_z^2 + k^2)e^{-jk|z-z'|} = -2jk\delta(z-z')$ . It follows then,

$$\begin{aligned} -4\pi jk\rho H_\phi(z, \rho) &= \int_{-h}^h I(z') (\partial_z^2 + k^2) e^{-jkR} dz' \rightarrow \int_{-h}^h I(z') (\partial_z^2 + k^2) e^{-jk|z-z'|} dz' \\ &= -2jk \int_{-h}^h I(z') \delta(z-z') dz' = -2jkI(z) \end{aligned}$$

or, for small  $\rho$ ,

$$H_\phi(z, \rho) = \frac{I(z)}{2\pi\rho} \quad (25.2.13)$$

Let  $Q(z)$  denote the charge density per unit  $z$ -length along the antenna, which is related to  $I(z)$  via the charge conservation equation  $I'(z) + j\omega Q(z) = 0$ . Then, the  $E_\rho$

component can be obtained from Maxwell's equation:

$$j\omega\epsilon E_\rho = -\partial_z H_\phi = -\frac{I'(z)}{2\pi\rho} = \frac{j\omega Q(z)}{2\pi\rho}$$

that is, for small  $\rho$ :

$$E_\rho(z, \rho) = \frac{Q(z)}{2\pi\epsilon\rho} \quad (25.2.14)$$

The same result can also be derived from Eq. (25.2.10) by recognizing the small- $\rho$  limit  $(z-z')e^{-jkR}/R \rightarrow \text{sign}(z-z')e^{-jk|z-z'|}$ , which satisfies the Helmholtz identity:

$$(\partial_z^2 + k^2)\text{sign}(z-z')e^{-jk|z-z'|} = 2\partial_z\delta(z-z')$$

Combining Eqs. (25.2.13) and (25.2.14) into the Faraday equation (25.2.12), we have,

$$\partial_\rho E_z = \partial_z E_\rho + j\omega\mu H_\phi = \frac{Q'(z)}{2\pi\epsilon\rho} + j\omega\mu \frac{I(z)}{2\pi\rho} = \frac{j}{\omega\epsilon} \frac{I''(z) + k^2 I(z)}{2\pi\rho}$$

Integrating from  $\rho = a$ , we obtain the small- $\rho$  King-Wu approximation:

$$E_z(z, \rho) = E_z(z, a) + \frac{j}{2\pi\omega\epsilon} [I''(z) + k^2 I(z)] \ln\left(\frac{\rho}{a}\right) \quad (25.2.15)$$

Strictly speaking, we must set  $E_z(z, a) = 0$  because of the boundary condition. However, in our numerical solution, we have kept the term  $E_z(z, a)$ , which is small but not necessarily exactly zero, in order to compare the analytical calculation (25.2.15) with the numerical solution. The left middle-row graphs confirm the linear dependence on  $\ln(\rho/a)$  with the right slope.

For longer antennas, up to about  $l = 3\lambda$ , the four-term approximation discussed in Sec. 24.6 can be used and leads to similar results. In this case, the following current expressions should be used:

$$I(z) = A_1 [\sin(k|z|) - \sin(kh)] + A_2 [\cos(kz) - \cos(kh)] +$$

$$+ A_3 \left[ \cos\left(\frac{kz}{4}\right) - \cos\left(\frac{kh}{4}\right) \right] + A_4 \left[ \cos\left(\frac{3kz}{4}\right) - \cos\left(\frac{3kh}{4}\right) \right]$$

$$I''(z') + k^2 I(z') = -k^2 A_1 \sin kh - k^2 A_2 \cos kh - k^2 A_3 \left[ \cos\left(\frac{kh}{4}\right) - \frac{15}{16} \cos\left(\frac{kz'}{4}\right) \right]$$

$$- k^2 A_4 \left[ \cos\left(\frac{3kh}{4}\right) - \frac{7}{16} \cos\left(\frac{3kz'}{4}\right) \right]$$

$$I'(0+) = -I'(0-) = kA_1$$

$$I'(h) = -I'(-h) = kA_1 \cos kh - kA_2 \sin kh - \frac{1}{4}kA_3 \sin\left(\frac{kh}{4}\right) - \frac{3}{4}kA_4 \sin\left(\frac{3kh}{4}\right)$$

We observe in the upper-right figures that the maximum values of  $|E_z(z, \rho)|$  occur roughly at distance:

$$\rho = \frac{\lambda}{20} \quad (25.2.16)$$

and this remains roughly true for antenna lengths  $0.5 \leq l/\lambda \leq 1.3$  and radii  $0.001 \leq a/\lambda \leq 0.007$  and for a variety of distances along the antenna, such as,  $0.2h \leq z \leq 0.7h$ .

Thus, this distance may be taken as a rough measure of the distance beyond which the standard terms begin to take over and the sinusoidal current approximation becomes justified.

The mutual impedance formulas that we develop in succeeding sections are based on the sinusoidal assumption, and therefore, they can be used more reliably for antenna separations  $d$  that are greater than that of Eq. (25.2.16). For example, to increase one's confidence, one could take the separations to be greater than, say, double the above value, that is,  $d \geq \lambda/10$ .

### 25.3 Self and Mutual Impedance

The mutual coupling between antennas cannot be ignored if the antennas are near each other. The *mutual impedance* is a measure of such proximity effects [2,1799-1811].

Consider two parallel center-driven linear dipoles, as shown in Fig. 25.3.1. Their distance along the  $x$ -direction is  $d$  and their centers are offset by  $b$  along the  $z$ -direction.

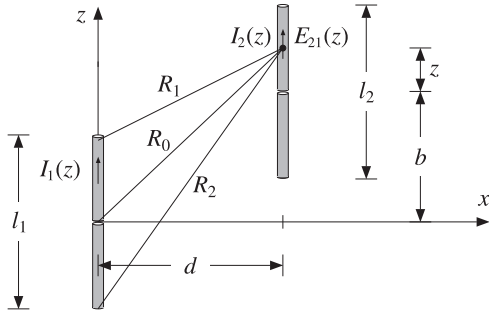


Fig. 25.3.1 Parallel linear dipoles.

If antenna-1 is driven and antenna-2 is open-circuited, the near field generated by the current on antenna-1 will cause an open-circuit voltage, say  $V_{21,oc}$  on antenna-2. The mutual impedance of antenna-2 due to antenna-1 is defined to be:

$$Z_{21} = \frac{V_{21,oc}}{I_1} \tag{25.3.1}$$

where  $I_1$  is the input current on antenna-1. Reciprocity implies that  $Z_{12} = Z_{21}$ . More generally, if both antennas are driven, then, the relationship of the driving voltages to the input currents is given by:

$$\begin{cases} V_1 = Z_{11}I_1 + Z_{12}I_2 \\ V_2 = Z_{21}I_1 + Z_{22}I_2 \end{cases} \tag{25.3.2}$$

The quantities  $Z_{11}, Z_{22}$  are the *self impedances* of the two antennas and are approximately equal to the input impedances of the isolated antennas, that is, when the other antenna is absent. If antenna-2 is open-circuited, so that  $I_2 = 0$ , then the second of Eqs. (25.3.2) gives (25.3.1).

In order to derive convenient expressions that allow the calculation of the mutual and self impedances, we use the reciprocity result given in Eq. (24.5.6) for the short-circuit current and open-circuit voltage induced on a receiving antenna in the presence of an incident field.

If antenna-2 is open-circuited and the  $z$ -component of the electric field generated by antenna-1 and incident on antenna-2 is  $E_{21}(z)$ , then according to Eq. (24.5.6), the induced open-circuit voltage will be:

$$V_{21,oc} = -\frac{1}{I_2} \int_{-h_2}^{h_2} E_{21}(z) I_2(z) dz \tag{25.3.3}$$

where  $h_2 = l_2/2$ , and  $I_2(z), I_2 = I_2(0)$  are the current and input current on antenna-2 when it is transmitting. It follows from definition (25.3.1) that:

$$Z_{21} = \frac{V_{21,oc}}{I_1} = -\frac{1}{I_1 I_2} \int_{-h_2}^{h_2} E_{21}(z) I_2(z) dz \tag{25.3.4}$$

Assuming that the currents are sinusoidal,

$$I_1(z) = I_1 \frac{\sin(k(h_1 - |z|))}{\sin kh_1} = I_{m1} \sin(k(h_1 - |z|))$$

$$I_2(z) = I_2 \frac{\sin(k(h_2 - |z|))}{\sin kh_2} = I_{m2} \sin(k(h_2 - |z|))$$

then, according to Eq. (25.1.9) the electric field  $E_{21}(z)$  along antenna-2 will be:

$$E_z(z) = -\frac{j\eta I_{m1}}{4\pi} \left[ \frac{e^{-jkR_1}}{R_1} + \frac{e^{-jkR_2}}{R_2} - 2 \cos kh_1 \frac{e^{-jkR_0}}{R_0} \right] \tag{25.3.5}$$

where  $-h_2 \leq z \leq h_2$ , and  $R_1, R_2, R_0$  are defined in Fig. 25.3.1:

$$\begin{aligned} R_0 &= \sqrt{d^2 + (z + b)^2} \\ R_1 &= \sqrt{d^2 + (z + b - h_1)^2} \\ R_2 &= \sqrt{d^2 + (z + b + h_1)^2} \end{aligned} \tag{25.3.6}$$

Inserting Eq. (25.3.5) into (25.3.4) and rearranging some constants, we find the final expression for the mutual impedance  $Z_{21}$ :

$$Z_{21} = \frac{j\eta}{4\pi \sin kh_1 \sin kh_2} \int_{-h_2}^{h_2} F(z) dz \tag{25.3.7}$$



$$F(z) = \left[ \frac{e^{-jkR_1}}{R_1} + \frac{e^{-jkR_2}}{R_2} - 2 \cos kh_1 \frac{e^{-jkR_0}}{R_0} \right] \sin(k(h_2 - |z|)) \quad (25.3.8)$$

This is the mutual impedance referred to the *input terminals* of the antennas. If one or both of the antennas have lengths that are multiples of  $\lambda$ , then one or both of the denominator factors  $\sin kh_1, \sin kh_2$  will vanish resulting in an infinite value for the mutual impedance.

This limitation is caused by the sinusoidal current assumption. We saw in Chap. 24 that the actual input currents are not zero in a real antenna. On the other hand, in most applications of Eq. (25.3.7) the lengths differ slightly from half-wavelength for which the sinusoidal approximation is good.

The definition (25.3.4) can also be referred to the *maximum currents* by normalizing by the factor  $I_{m1}I_{m2}$ , instead of  $I_1I_2$ . In this case, the mutual impedance is  $Z_{21m} = Z_{21} \sin kh_1 \sin kh_2$ , that is,

$$Z_{21m} = \frac{j\eta}{4\pi} \int_{-h_2}^{h_2} F(z) dz \quad (25.3.9)$$

The *self-impedance* of a single antenna can be calculated also by the same formula (25.3.7). Evaluating the near-field on the surface of the single antenna, that is, at  $d = a$ , where  $a$  is the antenna radius, and setting  $h_2 = h_1$  and  $b = 0$  in Eq. (25.3.6), we find:

$$Z_{11} = -\frac{1}{I_1^2} \int_{-h_1}^{h_1} E_{11}(z) I_1(z) dz = \frac{j\eta}{4\pi \sin^2 kh_1} \int_{-h_1}^{h_1} F(z) dz \quad (25.3.10)$$

$$F(z) = \left[ \frac{e^{-jkR_1}}{R_1} + \frac{e^{-jkR_2}}{R_2} - 2 \cos kh_1 \frac{e^{-jkR_0}}{R_0} \right] \sin(k(h_1 - |z|)) \quad (25.3.11)$$

$$R_0 = \sqrt{a^2 + z^2}, \quad R_1 = \sqrt{a^2 + (z - h_1)^2}, \quad R_2 = \sqrt{a^2 + (z + h_1)^2} \quad (25.3.12)$$

The MATLAB function `imped` implements Eq. (25.3.7), as well as (25.3.10). It returns both  $Z_{21}$  and  $Z_{21m}$  and has usage:

```
[Z21, Z21m] = imped(L2, L1, d, b)    % mutual impedance of dipole 2 due to dipole 1
[Z21, Z21m] = imped(L2, L1, d)    % b = 0, side-by-side arrangement
[Z, Zm] = imped(L, a)             % self impedance
```

where all the lengths are in units of  $\lambda$ . The function uses 16-point Gauss-Legendre integration, implemented with the help of the function `quadr`, to perform the integral in Eq. (25.3.7).

In evaluating the self impedance of an antenna with a small radius, the integrand  $F(z)$  varies rapidly around  $z = 0$ . To maintain accuracy in the integration, we split the integration interval into three subintervals, as we mentioned in Sec. 24.10.

**Example 25.3.1:** Because the function `imped` uses an even length (that is, 16) for the Gauss-Legendre integration, the integrand  $F(z)$  is never evaluated at  $z = 0$ , even if the antenna

radius is zero. This allows us to estimate the self-impedance of an infinitely thin half-wavelength antenna by setting  $L = 0.5$  and  $a = 0$ :

$$Z = \text{imped}(0.5, 0) = 73.0790 + 42.5151j \quad \Omega$$

Similarly, for radii  $a = 0.001\lambda$  and  $0.005\lambda$ , we find:

$$Z = \text{imped}(0.5, 0.001) = 73.0784 + 42.2107j \quad \Omega$$

$$Z = \text{imped}(0.5, 0.005) = 73.0642 + 40.6319j \quad \Omega$$

A resonant antenna is obtained by adjusting the length  $L$  such that the reactance part of  $Z$  becomes zero. The resonant length depends on the antenna radius. For zero radius, this length is  $L = 0.48574823$  and the corresponding impedance,  $Z = 67.1843 \quad \Omega$ .  $\square$

**Example 25.3.2:** Consider two identical parallel half-wavelength dipoles in side-by-side arrangement separated by distance  $d$ . The antenna radius is  $a = 0.001$  and therefore, its self impedance is as in the previous example. If antenna-1 is driven and antenna-2 is parasitic, that is, short-circuited, then Eq. (25.3.2) gives:

$$V_1 = Z_{11}I_1 + Z_{12}I_2$$

$$0 = Z_{21}I_1 + Z_{22}I_2$$

Solving the second for the parasitic current  $I_2 = -I_1 Z_{21}/Z_{22}$  and substituting in the first, we obtain driving-point impedance of the first antenna:

$$Z_{in} = \frac{V_1}{I_1} = Z_{11} - \frac{Z_{12}Z_{21}}{Z_{22}} = Z_{11} \left( 1 - \frac{Z_{21}^2}{Z_{11}^2} \right)$$

where we used  $Z_{12} = Z_{21}$  and  $Z_{22} = Z_{11}$ . The ratio  $Z_{21}^2/Z_{11}^2$  quantifies the effect of the coupling and the deviation of  $Z_{in}$  from  $Z_{11}$ . For example, we find the values:

$d$	0.125 $\lambda$	0.25 $\lambda$	0.50 $\lambda$	0.75 $\lambda$	1.00 $\lambda$
$ Z_{21}/Z_{11} ^2$	0.58	0.35	0.15	0.08	0.05

Thus, the ratio decreases rapidly with increasing distance  $d$ . Fig. 25.3.2 shows a plot of  $Z_{21}$  versus distance  $d$ .  $\square$

For separations  $d$  that are much larger than the antenna lengths, the impedance  $Z_{21}$  falls like  $1/d$ . Indeed, it follows from Eq. (25.3.6) that for large  $d$ , all three distances  $R_0, R_1, R_2$  become equal to  $d$ . Therefore, (25.3.8) tends to:

$$F(z) \rightarrow \frac{e^{-jkd}}{d} (2 - 2 \cos kh_1) \sin(k(h_2 - |z|))$$

which, when inserted into (25.3.7), gives the asymptotic form:

$$Z_{21} \rightarrow \frac{j\eta(1 - \cos kh_1)(1 - \cos kh_2)}{\pi \sin kh_1 \sin kh_2} \frac{e^{-jkd}}{kd}, \quad \text{for large } d \quad (25.3.13)$$

The envelope of this asymptotic form was superimposed on the graph of Fig. 25.3.2. The oscillatory behavior of  $Z_{21}$  with distance is essentially due to the factor  $e^{-jkd}$ .



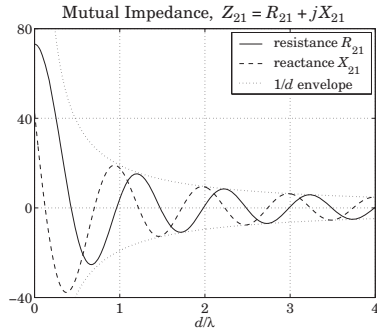


Fig. 25.3.2 Mutual impedance between identical half-wave dipoles vs. separation.

An alternative computation method of the mutual impedance is to reduce the integrals (25.3.7) to the exponential integral  $E_1(z)$  defined in Appendix F, taking advantage of MATLAB's built-in function `expint`.

By folding the integration range  $[-h_1, h_1]$  in half and writing  $\sin(k(h_2 - |z|))$  as a sum of exponentials, Eq. (25.3.7) can be reduced to a sum of terms of the form:

$$G(z_0, s) = \int_0^{h_1} \frac{e^{-jkR}}{R} e^{-jksz} dz, \quad R = \sqrt{d^2 + (z - z_0)^2}, \quad s = \pm 1 \quad (25.3.14)$$

which can be evaluated in terms of  $E_1(z)$  as:

$$G(z_0, s) = s e^{-jksz_0} [E_1(ju_0) - E_1(ju_1)] \quad (25.3.15)$$

with

$$u_0 = k \left[ \sqrt{d^2 + z_0^2} - sz_0 \right]$$

$$u_1 = k \left[ \sqrt{d^2 + (h_1 - z_0)^2} + s(h_1 - z_0) \right]$$

Indeed, the integral in (25.3.7) can be written as a linear combination of 10 such terms:

$$\int_{-h_1}^{h_1} F(z) dz = \sum_{i=1}^{10} c_i G(z_i, s_i) \quad (25.3.16)$$

with the following values of  $z_i$ ,  $c_i$ , and  $s_i$ , where  $c_1 = e^{jkh_2} / (2j)$ :

$i$	$z_i$	$s_i$	$c_i$	$i$	$z_i$	$s_i$	$c_i$
1	$h_1 - b$	1	$c_1$	6	$h_1 - b$	-1	$c_1^*$
2	$-h_1 + b$	1	$c_1$	7	$-h_1 + b$	-1	$c_1^*$
3	$-h_1 - b$	1	$c_1$	8	$-h_1 - b$	-1	$c_1^*$
4	$h_1 + b$	1	$c_1$	9	$h_1 + b$	-1	$c_1^*$
5	$b$	1	$-4c_1 \cos kh_1$	10	$b$	-1	$-4c_1^* \cos kh_1$

The MATLAB function `Gi` implements the "Green's function integral" of (25.3.14). The function `imped2`, which is an alternative to `imped`, uses (25.3.16) to calculate (25.3.7).

The input impedance (25.3.10) deserves a closer look. Replacing the exponential integrals in (25.3.16) in terms of their real and imaginary parts,

$$E_1(ju) = -\gamma - \ln u + C_{in}(u) + j(S_i(u) - \frac{\pi}{2})$$

as defined in Eq. (G.5), then (25.3.10) can be expressed in the following form, where we set  $Z_{11} = Z_{in} = R_{in} + jX_{in}$ ,  $h_1 = h$ , and  $l = 2h$ :

$$Z_{in} = R_{in} + jX_{in} = \frac{\eta}{2\pi} \frac{A + jB}{\sin^2 kh} \quad (25.3.17)$$

With the definitions  $l_{\pm} = \sqrt{a^2 + h^2} \pm h$  and  $L_{\pm} = \sqrt{a^2 + 4h^2} \pm 2h$ , we obtain:

$$A = C_{in}(kl_+) + C_{in}(kl_-) - 2C_{in}(ka)$$

$$+ \frac{1}{2} \cos kl [2C_{in}(kl_+) - C_{in}(kL_+) + 2C_{in}(kl_-) - C_{in}(kL_-) - 2C_{in}(ka)] \quad (25.3.18)$$

$$+ \frac{1}{2} \sin kl [2S_i(kl_-) - S_i(kL_-) + S_i(kL_+) - 2S_i(kl_+)]$$

$$B = S_i(kl_+) + S_i(kl_-) - 2S_i(ka)$$

$$+ \frac{1}{2} \cos kl [2S_i(kl_+) - S_i(kL_+) + 2S_i(kl_-) - S_i(kL_-) - 2S_i(ka)] \quad (25.3.19)$$

$$+ \frac{1}{2} \sin kl \left[ 2C_{in}(kl_+) - C_{in}(kL_+) + C_{in}(kL_-) - 2C_{in}(kl_-) + 2 \ln \left( \frac{aL_+}{l_+^2} \right) \right]$$

These expressions simplify substantially if we assume that the radius  $a$  is small, as is the case in practice. In particular, assuming that  $ka \ll 1$  and  $a \ll h$ , the quantities  $l_{\pm}$  and  $L_{\pm}$  can be approximated by:

$$l_+ \approx 2h = l, \quad l_- = \frac{a^2}{l_+} \approx \frac{a^2}{l} \quad (25.3.20)$$

$$L_+ \approx 4h = 2l, \quad L_- = \frac{a^2}{L_+} \approx \frac{a^2}{2l}$$

Noting that  $S_i(x)$  and  $C_{in}(x)$  vanish at  $x = 0$ , we may neglect all the terms whose arguments are  $kl_-$ ,  $kL_-$ , or  $ka$ , and replace  $kl_+ = kl$  and  $kL_+ = 2kl$ , obtaining:

$$A = C_{in}(kl) + \frac{1}{2} \cos kl [2C_{in}(kl) - C_{in}(2kl)] + \frac{1}{2} \sin kl [S_i(2kl) - 2S_i(kl)] \quad (25.3.21)$$

$$B = S_i(kl) + \frac{1}{2} \cos kl [2S_i(kl) - S_i(2kl)] + \frac{1}{2} \sin kl \left[ 2C_{in}(kl) - C_{in}(2kl) + 2 \ln \left( \frac{2a}{l} \right) \right] \quad (25.3.22)$$

We note that  $A$  is independent of the radius  $a$  and leads to the same expression for the radiation resistance that we found in Sec. 17.3 using Poynting methods.

An additional approximation can be made for the case of a *small dipole*. Assuming that  $kh \ll 1$ , in addition to  $ka \ll 1$  and  $a \ll h$ , we may expand each of the above terms

into a Taylor series in the variable  $kh$  using the following Taylor series expansions of the functions  $S_i(x)$  and  $C_{in}(x)$ :

$$S_i(x) \approx x - \frac{1}{18}x^3 + \frac{1}{600}x^5, \quad C_{in}(x) \approx \frac{1}{4}x^2 - \frac{1}{96}x^4 + \frac{1}{4320}x^6 \quad (25.3.23)$$

Such expansions, lead to the following input impedance  $Z = R + jX$  to the lowest non-trivial order in  $kl$ :

$$Z_{in} = R_{in} + jX_{in} = \frac{\eta}{2\pi} \left[ \frac{1}{12}(kl)^2 + j\frac{4(1+L)}{kl} \right] \quad (\text{small dipole}) \quad (25.3.24)$$

where  $L = \ln(2a/l)$ . The resistance  $R$  is identical to that obtained using the Poynting method and assuming a linear approximation to the sinusoidal antenna current, which is justified when  $kh \ll 1$ :

$$I(z) = I_0 \frac{\sin(k(h - |z|))}{\sin kh} \approx I_0 \frac{k(h - |z|)}{kh} = I_0 \left( 1 - \frac{|z|}{h} \right) \quad (25.3.25)$$

### 25.4 Coupled Two-Element Arrays

Next, we consider a more precise justification of Eq. (25.3.2) and generalize it to the case of an arbitrary array of parallel linear antennas. Fig. 25.4.1 shows two  $z$ -directed parallel dipoles with centers at locations  $(x_1, y_1)$  and  $(x_2, y_2)$ .

We assume that the dipoles are center-driven by the voltage generators  $V_1, V_2$ . Let  $I_1(z), I_2(z)$  be the currents induced on the dipoles by the generators and by their mutual interaction, and let  $h_1, h_2$  be the half-lengths of the antennas, and  $a_1, a_2$ , their radii. Then, assuming the thin-wire model, the total current density will have only a  $z$ -component given by:

$$J_z(x', y', z') = I_1(z') \delta(x' - x_1) \delta(y' - y_1) + I_2(z') \delta(x' - x_2) \delta(y' - y_2) \quad (25.4.1)$$

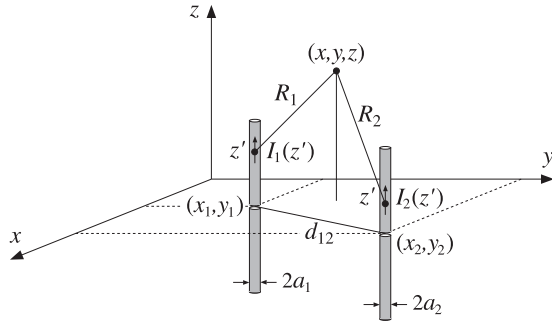


Fig. 25.4.1 Array of two linear antennas.

It follows that the magnetic vector potential will be:

$$A_z(z, \boldsymbol{\rho}) = \frac{\mu}{4\pi} \int \frac{e^{-jkR}}{R} J_z(x', y', z') dx' dy' dz', \quad R = |\mathbf{r} - \mathbf{r}'|$$

where  $\boldsymbol{\rho} = x\hat{\mathbf{x}} + y\hat{\mathbf{y}}$  is the cylindrical radial vector. Inserting (25.4.1) and performing the  $x', y'$  integrations, we obtain:

$$A_z(z, \boldsymbol{\rho}) = \frac{\mu}{4\pi} \int_{-h_1}^{h_1} \frac{e^{-jkR_1}}{R_1} I_1(z') dz' + \frac{\mu}{4\pi} \int_{-h_2}^{h_2} \frac{e^{-jkR_2}}{R_2} I_2(z') dz' \quad (25.4.2)$$

where, as shown in Fig. 25.4.1,  $R_1, R_2$  are the distances from the  $z'$  point on each antenna to the  $(x, y, z)$  observation point, that is,

$$R_1 = \sqrt{(z - z')^2 + (x - x_1)^2 + (y - y_1)^2} = \sqrt{(z - z')^2 + |\boldsymbol{\rho} - \mathbf{d}_1|^2} \\ R_2 = \sqrt{(z - z')^2 + (x - x_2)^2 + (y - y_2)^2} = \sqrt{(z - z')^2 + |\boldsymbol{\rho} - \mathbf{d}_2|^2} \quad (25.4.3)$$

where  $\mathbf{d}_1 = (x_1, y_1)$  and  $\mathbf{d}_2 = (x_2, y_2)$  are the  $xy$ -locations of the antenna centers. The  $z$ -component of the electric field generated by the two antenna currents will be:

$$j\omega\epsilon\mu E_z(z, \boldsymbol{\rho}) = (\partial_z^2 + k^2) A_z(z, \boldsymbol{\rho})$$

Working with the rescaled vector potential  $V(z, \boldsymbol{\rho}) = 2j\epsilon A_z(z, \boldsymbol{\rho})$ , we rewrite:

$$V(z, \boldsymbol{\rho}) = \frac{j\eta}{2\pi} \int_{-h_1}^{h_1} \frac{e^{-jkR_1}}{R_1} I_1(z') dz' + \frac{j\eta}{2\pi} \int_{-h_2}^{h_2} \frac{e^{-jkR_2}}{R_2} I_2(z') dz' \quad (25.4.4)$$

$$(\partial_z^2 + k^2) V(z, \boldsymbol{\rho}) = -2kE_z(z, \boldsymbol{\rho}) \quad (25.4.5)$$

Denoting by  $V_1(z)$  and  $V_2(z)$  the values of  $V(x, y, z)$  on the surfaces of antenna-1 and antenna-2, we obtain from Eq. (25.4.4):

$$V_1(z) = V_{11}(z) + V_{12}(z) \\ V_2(z) = V_{21}(z) + V_{22}(z) \quad (25.4.6)$$

The  $z$ -components of the electric fields induced on the surfaces of antenna-1 and antenna-2 are obtained by applying Eq. (25.4.5) to each term of (25.4.6):

$$E_1(z) = E_{11}(z) + E_{12}(z) \\ E_2(z) = E_{21}(z) + E_{22}(z) \quad (25.4.7)$$

where we defined, for  $p, q = 1, 2$ :

$$V_{pq}(z) = \frac{j\eta}{2\pi} \int_{-h_q}^{h_q} G_{pq}(z - z') I_q(z') dz' \\ (\partial_z^2 + k^2) V_{pq}(z) = -2kE_{pq}(z) \quad (25.4.8)$$

and the impedance kernels:

$$G_{pq}(z - z') = \frac{e^{-jkR_{pq}}}{R_{pq}}, \quad R_{pq} = \sqrt{(z - z')^2 + d_{pq}^2} \quad (25.4.9)$$

If  $p \neq q$ , then  $d_{pq}$  is the  $xy$ -distance between the antennas, and if  $p = q$ , it is the radius of the corresponding antenna, that is,

$$d_{12} = d_{21} = |\mathbf{d}_1 - \mathbf{d}_2| = \sqrt{(x_1 - x_2)^2 + (y_1 - y_2)^2}$$

$$d_{11} = a_1, \quad d_{22} = a_2$$
(25.4.10)

Thus,  $V_{pq}(z)$  and  $E_{pq}(z)$  are the vector potential and the  $z$ -component of the electric field induced on antenna- $p$  by the current  $I_q(z)$  on antenna- $q$ .

To clarify these definitions, Fig. 25.4.2 shows a projected view of Fig. 25.4.1 on the  $xy$  plane. The point  $P$  with radial vector  $\boldsymbol{\rho}$  is the projection of the observation point  $(z, \boldsymbol{\rho})$ . When  $P$  coincides with a point, such as  $P_2$ , on the surface of antenna-2 defined by the radial vector  $\boldsymbol{\rho}_2$ , then the distance  $(P_2O_2) = |\boldsymbol{\rho}_2 - \mathbf{d}_2|$  will be equal to the antenna radius  $a_2$ , regardless of the location of  $P_2$  around the periphery of the antenna.

On the other hand, the distance  $(P_2O_1) = |\boldsymbol{\rho}_2 - \mathbf{d}_1|$  varies with  $P_2$ . However, because the separation  $d_{12}$  is typically  $d_{12} \gg a_2$ , such variation is minor and we may replace  $|\boldsymbol{\rho}_2 - \mathbf{d}_1|$  by  $|\mathbf{d}_2 - \mathbf{d}_1|$ . Thus, in evaluating  $V(z, \boldsymbol{\rho}_2)$  on antenna-2, we may use Eq. (25.4.4) with  $R_1, R_2$  defined by:

$$R_1 = \sqrt{(z - z')^2 + |\mathbf{d}_2 - \mathbf{d}_1|^2} = \sqrt{(z - z')^2 + d_{12}^2}$$

$$R_2 = \sqrt{(z - z')^2 + |\boldsymbol{\rho}_2 - \mathbf{d}_2|^2} = \sqrt{(z - z')^2 + a_2^2}$$
(25.4.11)

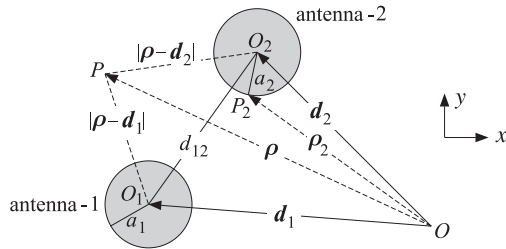


Fig. 25.4.2 Array of two linear antennas.

Now, on the surface of the first antenna, the electric field  $E_z$  must cancel the field of the delta-gap generator in order for the total tangential field to vanish, that is,  $E_1(z) = -E_{1,\text{in}}(z) = -V_1\delta(z)$ . Similarly, on the surface of the second antenna, we must have  $E_2(z) = -E_{2,\text{in}}(z) = -V_2\delta(z)$ . Then, Eq. (25.4.7) becomes:

$$E_{11}(z) + E_{12}(z) = E_1(z) = -V_1\delta(z)$$

$$E_{21}(z) + E_{22}(z) = E_2(z) = -V_2\delta(z)$$
(25.4.12)

Combining these with the Eq. (25.4.8), we obtain the coupled version of the Hallén-Pocklington equations:

$$(\partial_z^2 + k^2) [V_{11}(z) + V_{12}(z)] = 2kV_1\delta(z)$$

$$(\partial_z^2 + k^2) [V_{21}(z) + V_{22}(z)] = 2kV_2\delta(z)$$
(25.4.13)

We will solve these numerically in Sec. 25.7. Next, we derive Eq. (25.3.2). According to definitions (25.3.4) and (25.3.10), the mutual impedance between antenna- $p$  and antenna- $q$  can be restated as follows, for  $p, q = 1, 2$ :

$$Z_{pq} = -\frac{1}{I_p I_q} \int_{-h_p}^{h_p} E_{pq}(z) I_p(z) dz$$
(25.4.14)

and, more explicitly:

$$Z_{11} = -\frac{1}{I_1 I_1} \int_{-h_1}^{h_1} E_{11}(z) I_1(z) dz, \quad Z_{12} = -\frac{1}{I_1 I_2} \int_{-h_1}^{h_1} E_{12}(z) I_1(z) dz$$

$$Z_{21} = -\frac{1}{I_2 I_1} \int_{-h_2}^{h_2} E_{21}(z) I_2(z) dz, \quad Z_{22} = -\frac{1}{I_2 I_2} \int_{-h_2}^{h_2} E_{22}(z) I_2(z) dz$$

Using these definitions and Eq. (25.4.12), we find:

$$Z_{11} I_1 + Z_{12} I_2 = -\frac{1}{I_1} \int_{-h_1}^{h_1} [E_{11}(z) + E_{12}(z)] I_1(z) dz$$

$$= -\frac{1}{I_1} \int_{-h_1}^{h_1} [-V_1 \delta(z)] I_1(z) dz = \frac{1}{I_1} V_1 I_1(0) = V_1$$

where, by definition,  $I_1(0) = I_1$ . Similarly, we can show the second of Eq. (25.3.2).

The mutual impedance defined in Eq. (25.4.14) actually satisfies the reciprocity symmetry condition,  $Z_{pq} = Z_{qp}$ . To write it in a form that shows this condition explicitly, we replace  $E_{pq}(z)$  by (25.4.8) and obtain the alternative symmetric form:

$$Z_{pq} = \frac{j\eta}{4\pi k} \int_{-h_p}^{h_p} \int_{-h_q}^{h_q} \frac{I_p(z) I_q(z')}{I_p I_q} (\partial_z^2 + k^2) G_{pq}(z - z') dz dz'$$
(25.4.15)

If we assume that the currents are sinusoidal, that is, for  $p = 1, 2$ ,

$$I_p(z) = I_p \frac{\sin(k(h_p - |z|))}{\sin kh_p}$$
(25.4.16)

then, in Eq. (25.4.15) the ratios  $I_p(z)/I_p$  and hence  $Z_{pq}$  become independent of the input currents at the antenna terminals and depend only on the geometry of the antennas.

### 25.5 Arrays of Parallel Dipoles

The above results on two antennas generalize in a straightforward fashion to several antennas. Fig. 25.5.1 depicts the case of  $K$  parallel dipoles in side-by-side arrangement with centers at positions  $(x_p, y_p)$ , and driving voltages, lengths, half-lengths, and radii,  $V_p, l_p, h_p, a_p$ , where  $p = 1, 2, \dots, K$ .

Assuming sinusoidal currents as in Eq. (25.4.16), we define the mutual impedances  $Z_{pq}$  by Eq. (25.4.14) or (25.4.15), where  $p, q$  take on the values  $p, q = 1, 2, \dots, K$ . The

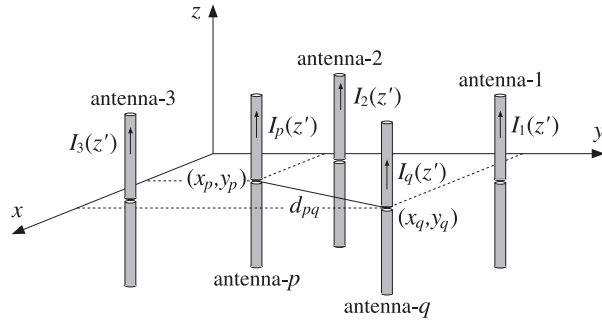


Fig. 25.5.1 Two-dimensional array of parallel dipoles.

Hallén-Pocklington equations (25.4.13) generalize into:

$$(\partial_z^2 + k^2) \sum_{q=1}^K V_{pq}(z) = -2k \sum_{q=1}^K E_{pq}(z) = 2kV_p \delta(z), \quad p = 1, 2, \dots, K \quad (25.5.1)$$

where  $V_{pq}(z)$  is defined by Eqs. (25.4.8) and (25.4.9). The mutual distances are:

$$d_{pq} = \begin{cases} \sqrt{(x_p - x_q)^2 + (y_p - y_q)^2}, & \text{if } p \neq q \\ a_p, & \text{if } p = q \end{cases} \quad (25.5.2)$$

Multiplying Eq. (25.5.1) by  $I_p(z)$  and integrating along the length of the  $p$ th antenna, and using the mutual impedance definitions (25.4.14), we obtain the generalization of Eq. (25.3.2) to the case of  $K$  antennas:

$$V_p = \sum_{q=1}^K Z_{pq} I_q, \quad p = 1, 2, \dots, K \quad (25.5.3)$$

where  $I_q$  is the input current at the center of the  $q$ th antenna. Eq. (25.5.3) may be written in a compact matrix form:

$$\mathbf{V} = \mathbf{Z} \mathbf{I} \quad (25.5.4)$$

where  $\mathbf{Z}$  is the *impedance matrix*. For example, in the case  $K = 4$ , we have:

$$\mathbf{V} = \begin{bmatrix} V_1 \\ V_2 \\ V_3 \\ V_4 \end{bmatrix} = \begin{bmatrix} Z_{11} & Z_{12} & Z_{13} & Z_{14} \\ Z_{21} & Z_{22} & Z_{23} & Z_{24} \\ Z_{31} & Z_{32} & Z_{33} & Z_{34} \\ Z_{41} & Z_{42} & Z_{43} & Z_{44} \end{bmatrix} \begin{bmatrix} I_1 \\ I_2 \\ I_3 \\ I_4 \end{bmatrix} = \mathbf{Z} \mathbf{I}$$

We note that  $\mathbf{Z}$  is a symmetric matrix,  $\mathbf{Z} = \mathbf{Z}^T$ , as a consequence of the reciprocity relations  $Z_{pq} = Z_{qp}$ .

Given the driving voltages  $V_p$ , Eq. (25.5.4) may be solved for the input currents  $I_p$ , which completely define the assumed sinusoidal currents  $I_p(z)$  of Eq. (25.4.16). From

the knowledge of the currents  $I_p(z)$ , one can obtain the radiation pattern of the array. Indeed, the radiation fields are obtained from Eq. (17.1.6), that is,

$$\begin{aligned} \mathbf{E} &= \hat{\boldsymbol{\theta}} E_\theta = \hat{\boldsymbol{\theta}} jk\eta \frac{e^{-jkr}}{4\pi r} F_z(\theta, \phi) \sin \theta \\ \mathbf{H} &= \hat{\boldsymbol{\phi}} H_\phi = \hat{\boldsymbol{\phi}} jk \frac{e^{-jkr}}{4\pi r} F_z(\theta, \phi) \sin \theta \end{aligned} \quad (25.5.5)$$

where the radiation vector  $\mathbf{F} = \hat{\mathbf{z}} F_z$  has only a  $z$ -component given by:

$$F_z(\theta, \phi) = \int_{V'} J_z(\mathbf{r}') e^{jk \cdot \mathbf{r}'} d\mathbf{r}' \quad (25.5.6)$$

But, in the thin-wire approximation, the total current density of the array is:

$$J_z(\mathbf{r}') = \sum_{p=1}^K I_p(z') \delta(x' - x_p) \delta(y' - y_p)$$

Inserting this into Eq. (25.5.6) and performing the  $x', y'$  integrations, we obtain:

$$F_z(\theta, \phi) = \sum_{p=1}^K e^{jk_x x_p + jk_y y_p} \int_{-h_p}^{h_p} I_p(z') e^{jk_z z'} dz' \quad (25.5.7)$$

Using Eq. (25.4.16) for  $I_p(z)$  and replacing  $k_z = k \cos \theta$ , we obtain:

$$F_z(\theta, \phi) = \sum_{p=1}^K e^{jk_x x_p + jk_y y_p} \frac{2I_p}{k \sin kh_p} \frac{\cos(kh_p \cos \theta) - \cos kh_p}{\sin^2 \theta} \quad (25.5.8)$$

The radiation intensity is given, in general, by Eq. (16.1.4):

$$U(\theta, \phi) = \frac{\eta k^2}{32\pi^2} |\sin \theta F_z(\theta, \phi)|^2$$

Replacing  $k_x = k \sin \theta \cos \phi$  and  $k_y = k \sin \theta \sin \phi$ , we obtain:

$$U(\theta, \phi) = \frac{\eta}{8\pi^2} \left| \sum_{p=1}^K I_p \frac{\cos(kh_p \cos \theta) - \cos kh_p}{\sin kh_p \sin \theta} e^{jk \sin \theta (x_p \cos \phi + y_p \sin \phi)} \right|^2$$

Thus, the normalized *gain* of the array will be, up to a proportionality constant:

$$g(\theta, \phi) = \left| \sum_{p=1}^K I_p \frac{\cos(kh_p \cos \theta) - \cos kh_p}{\sin kh_p \sin \theta} e^{jk \sin \theta (x_p \cos \phi + y_p \sin \phi)} \right|^2 \quad (25.5.9)$$

Equations (25.5.4) and (25.5.9) provide a complete solution to the problem of coupled antenna arrays, based on the sinusoidal approximation for the currents. In the

special case of identical antennas, Eq. (25.5.9) factors as usual into an array factor and an element factor:

$$g(\theta, \phi) = \left| \sum_{p=1}^K I_p e^{jk \sin \theta (x_p \cos \phi + y_p \sin \phi)} \right|^2 \left| \frac{\cos(kh \cos \theta) - \cos kh}{\sin kh \sin \theta} \right|^2$$

The MATLAB function `impedmat` calculates the  $K \times K$  mutual impedance matrix  $Z$  of such an array, given the antenna lengths and radii,  $l_p, a_p$ , and the coordinates  $(x_p, y_p)$ , for  $p = 1, 2, \dots, K$ . It has usage:

```
Z = impedmat(L, a, d); % mutual impedance matrix of array of parallel dipoles
```

where all the lengths must be given in units of  $\lambda$ . It calls `imped` to calculate the individual matrix elements  $Z_{pq}$ .

The input parameters  $L, a, d$  are the vectors of antenna lengths, antenna radii, and  $(x_p, y_p)$  pairs, or the  $x_p$  positions, if the array is along the  $x$ -axis:

$$L = \begin{bmatrix} L_1 \\ L_2 \\ \vdots \\ L_K \end{bmatrix}, \quad a = \begin{bmatrix} a_1 \\ a_2 \\ \vdots \\ a_K \end{bmatrix}, \quad d = \begin{bmatrix} x_1, y_1 \\ x_2, y_2 \\ \vdots \\ x_K, y_K \end{bmatrix} \quad \text{or} \quad \begin{bmatrix} x_1 \\ x_2 \\ \vdots \\ x_K \end{bmatrix}$$

The MATLAB function `gain2s` calculates the  $E$ -plane and  $H$ -plane array gains using Eq. (25.5.9) and assumes that the input currents  $I_p$  have been obtained by solving Eq. (25.5.4). It has usage:

```
[ge, gh, th] = gain2s(L, d, I, N, ph0); % gain of 2D array of dipoles with sinusoidal currents
[ge, gh, th] = gain2s(L, d, I, N); % equivalent to ph0 = 0
```

where the input parameters  $L, a$  have the same meaning as in `impedmat`, and  $I$  is the vector of input currents  $I = [I_1, I_2, \dots, I_K]$ . The output angle parameter `th` is either the polar or the azimuthal angle and takes  $N$  equally-spaced values in the interval  $[0, 2\pi]$ .

The  $H$ -plane gain  $g_H(\phi)$  is defined to be the azimuthal gain on the  $xy$ -plane corresponding to  $\theta = \pi/2$ , and the  $E$ -plane gain  $g_E(\theta)$  is defined to be the polar gain on any fixed azimuthal plane  $\phi = \phi_0$ , that is,

$$\begin{cases} g_H(\phi) = g(\pi/2, \phi), & 0 \leq \phi \leq 2\pi \\ g_E(\theta) = g(\theta, \phi_0), & 0 \leq \theta \leq 2\pi \end{cases} \quad (25.5.10)$$

Note that by allowing  $\theta$  to vary over  $[0, 2\pi]$ , the  $E$ -plane gain can give both the forward and backward gain. The polar angle range  $[0, \pi]$  covers the forward direction  $\phi = \phi_0$ , whereas, the range  $[\pi, 2\pi]$  covers the backward direction  $\phi = \phi_0 + \pi$ , that is, we have the equivalence:

$$g(\theta, \phi_0) = g(\theta - \pi, \phi_0 + \pi), \quad \pi \leq \theta \leq 2\pi$$

This follows from the trigonometric identities:

$$\begin{aligned} \sin(\theta - \pi) \cos(\phi_0 + \pi) &= \sin \theta \cos \phi_0 \\ \sin(\theta - \pi) \sin(\phi_0 + \pi) &= \sin \theta \sin \phi_0 \end{aligned}$$

Because both gains are defined over a  $2\pi$ -angular range, they must be plotted with the MATLAB functions `abp2` and `abz2`, or in dB, with `dbp2` and `dbz2`.

**Example 25.5.1:** *Three-element parasitic array.* Undriven parasitic antennas located near transmitting ones can act as reflectors or directors, directing the radiation towards certain preferred directions. Fig. 25.5.2 shows an array of three half-wavelength dipoles. The geometry is the same as that of Example 22.3.3. The  $xy$ -coordinates of the elements are  $\mathbf{d}_1 = (0, 0)$ ,  $\mathbf{d}_2 = (0.5\lambda, 0)$ , and  $\mathbf{d}_3 = (0, 0.5\lambda)$ .

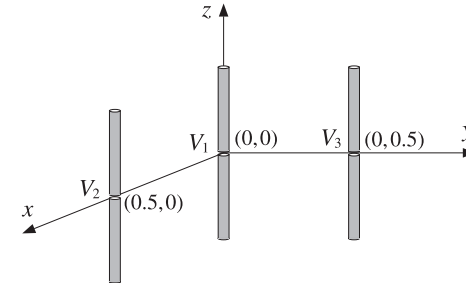


Fig. 25.5.2 Three-element array.

Let  $V = [V_1, V_2, V_3]^T$  be the driving voltages of the three elements. If only element-1 is driven and the others parasitic, we may take  $V = [1, 0, 0]^T$ .

If the mutual couplings between the antennas are ignored, that is, the impedance matrix  $Z$  of Eq. (25.5.4) is taken to be diagonal, then, the input currents, will be  $I = [I_1, 0, 0]$  and the parasitic elements will be completely passive as though they were absent. The radiation pattern would be that of a single half-wave dipole. In particular, the azimuthal pattern would be omnidirectional.

This is not the case if the mutual couplings are taken into account. The parasitic elements act as reflectors, reflecting the radiation back towards the active element-1. By the symmetry of the arrangement, the maximum directivity will be in the direction with azimuthal angle  $\phi = -135^\circ$ . Fig. 25.5.3 shows the resulting  $H$ -plane and  $E$ -plane radiation patterns demonstrating this behavior. The dashed gains were computed by solving the coupled system of Hallén equations for the exact currents on each of the three antennas, as discussed in Example 25.7.1.

Assuming equal radii,  $a = 0.001\lambda$ , the  $3 \times 3$  impedance matrix  $Z$  is found to be:

$$Z = \begin{bmatrix} 73.08 + 42.21j & -12.52 - 29.91j & -12.52 - 29.91j \\ -12.52 - 29.91j & 73.08 + 42.21j & -24.62 + 0.78j \\ -12.52 - 29.91j & -24.62 + 0.78j & 73.08 + 42.21j \end{bmatrix}$$

Then, the solution of Eq. (25.5.4) is:

$$I = \begin{bmatrix} I_1 \\ I_2 \\ I_3 \end{bmatrix} = Z^{-1}V = Z^{-1} \begin{bmatrix} 1 \\ 0 \\ 0 \end{bmatrix} = \begin{bmatrix} 0.0133 \angle -7.46^\circ \\ 0.0066 \angle 18.23^\circ \\ 0.0066 \angle 18.23^\circ \end{bmatrix}$$

The typical MATLAB code used to generate these graphs was as follows:

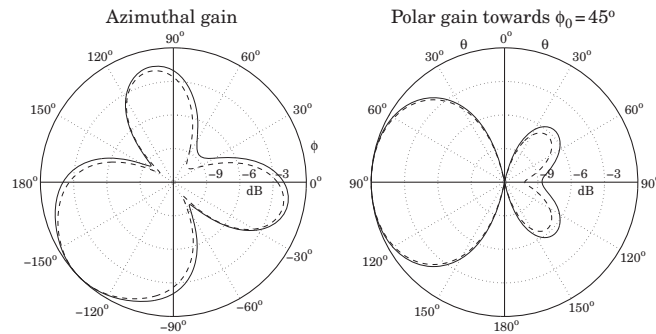


Fig. 25.5.3 H-plane and E-plane radiation patterns,  $V = [1, 0, 0]^T$ .

```

L = [0.5, 0.5, 0.5];           % lengths
a = [0.001, 0.001, 0.001];    % radii
d = [0, 0; 0.5, 0; 0, 0.5];    % xy locations

Z = impedmat(L, a, d);         % impedance matrix
V = [1; 0; 0];                 % driving voltages
I = Z \ V;                      % input currents

ph0 = 45;                       % 45° azimuthal plane for polar gain

[ge1, gh1, ph] = gain2s(L, d, I, 360, ph0); % gain2s assumes sinusoidal currents

M = 40;                          % number of upper-half samples

[I, z] = hcoupled2(L, a, d, V, M); % solves for currents on all antennas

[ge2, gh2, ph] = gain2d(L, d, I, 360, ph0); % gain2d uses Hallén currents

figure; dbz2(ph, gh1, 30, 12); dbadd2(2, '--', ph, gh2, 30, 12);
figure; dbp2(ph, ge1, 30, 12); dbadd2(1, '--', ph, ge2, 30, 12);
    
```

Anticipating the symmetry about the  $45^\circ$  azimuthal plane, the E-plane gain was computed with  $\phi_0 = 45^\circ$ . As expected, the polar plot shows that the maximum gain is in the backward  $\phi_0$  direction, that is, toward  $\phi_0 + 180^\circ = 225^\circ = -135^\circ$ . □

**Example 25.5.2:** Next, consider the case when element-one is parasitic, but elements two and three are driven by equal voltages,  $V = [0, 1, 1]^T$ . If the mutual coupling is ignored, then the two active elements act as an array which is broadside to the line joining them, that is, maximum directivity is in the  $45^\circ$  azimuthal direction, but with both the forward and the backward (i.e.,  $-135^\circ$ ) directions being equal. This pattern is shown in the upper-right graph of Fig. 22.3.4.

If the mutual couplings are taken into account, element-1 will act as a reflector, reflecting towards the  $\phi_0 = 45^\circ$  direction and reducing the gain in the opposite direction. This is demonstrated in Fig. 25.5.4. As in the previous example, the dashed gains correspond to the exact coupled Hallén solution.

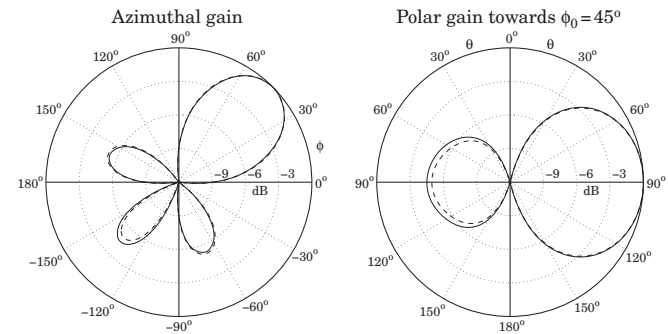


Fig. 25.5.4 H-plane and E-plane radiation patterns,  $V = [0, 1, 1]^T$ .

Because of the identical geometry, the impedance matrix  $Z$  is the same as that of the previous example. But, the input currents are different:

$$I = \begin{bmatrix} I_1 \\ I_2 \\ I_3 \end{bmatrix} = Z^{-1} V = Z^{-1} \begin{bmatrix} 0 \\ 1 \\ 1 \end{bmatrix} = \begin{bmatrix} 0.0133 \angle 18.23^\circ \\ 0.0173 \angle -19.04^\circ \\ 0.0173 \angle -19.04^\circ \end{bmatrix}$$

The only change in the previous MATLAB code was to use  $V = [0, 1, 1]^T$ . □

**Example 25.5.3:** One of the earliest experimental studies of parasitic reflectors was by Nagy [1803]. One of his arrangements is shown in Fig. 25.5.5 in which the driven element is at the origin and the other three elements are parasitic. The antenna lengths were  $l = 1.19$  m, and their radii  $a = 0.395$  cm. The operating wavelength was  $\lambda = 2.5$  meters, (i.e., frequency of 120 MHz.)

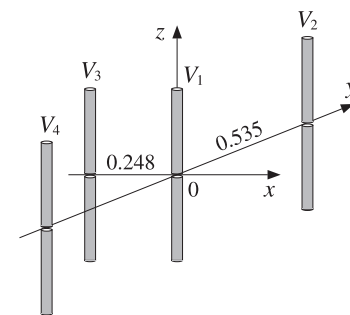


Fig. 25.5.5 Four-element parasitic array.

It follows that,  $l = 0.476\lambda$  and  $a = 0.00158\lambda$ . Elements two and four were placed symmetrically along the  $y$ -axis at distances  $\pm 0.535\lambda$ , and element three was on the negative side of the  $x$ -axis at distance  $0.248\lambda$  from the origin. Fig. 25.5.6 shows the calculated patterns. We observe that the three parasitic antennas act as reflectors, enhancing the radiation in the  $\phi = 0$  direction.

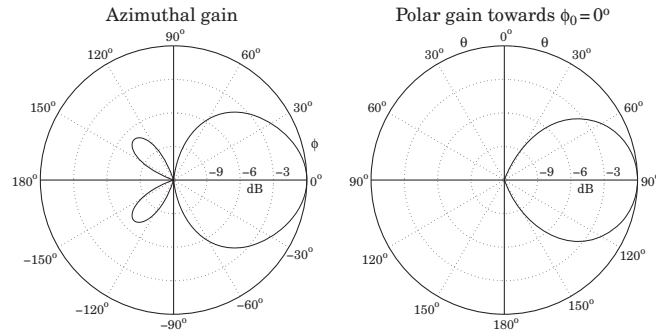


Fig. 25.5.6 H-plane and E-plane radiation patterns,  $V = [1, 0, 0, 0]^T$ .

This array was later studied theoretically by Brown [1804], using the same methods as those presented here. Brown treated monopole antennas (i.e. half dipoles above a ground plane,) and therefore, the values of his mutual impedances are half of ours. The inputs to the design equations were the parameters:

$$L = \begin{bmatrix} 0.476 \\ 0.476 \\ 0.476 \\ 0.476 \end{bmatrix}, \quad \mathbf{a} = \begin{bmatrix} 0.00158 \\ 0.00158 \\ 0.00158 \\ 0.00158 \end{bmatrix}, \quad \mathbf{d} = \begin{bmatrix} 0.000, & 0.000 \\ 0.000, & 0.535 \\ -0.248, & 0.000 \\ 0.000, & -0.535 \end{bmatrix}$$

The impedance matrix elements are:

$$\begin{aligned} Z_{11} = Z_{22} = Z_{33} &= 63.42 \angle 0.65^\circ, & Z_{12} = Z_{14} &= 26.76 \angle -123.87^\circ \\ Z_{13} &= 43.56 \angle -34.69^\circ, & Z_{23} = Z_{34} &= 24.78 \angle -141.96^\circ \\ Z_{24} &= 14.74 \angle 53.15^\circ \end{aligned}$$

With  $V = [1, 0, 0, 0]^T$ , the solution of  $ZI = V$  is:

$$I = \begin{bmatrix} I_1 \\ I_2 \\ I_3 \\ I_4 \end{bmatrix} = \begin{bmatrix} 0.0135 \angle -26.26^\circ \\ 0.0043 \angle 74.61^\circ \\ 0.0126 \angle 116.70^\circ \\ 0.0043 \angle 4.61^\circ \end{bmatrix}$$

and we find for the ratios:

$$\frac{I_2}{I_1} = \frac{I_4}{I_1} = 0.3180 \angle 100.87^\circ, \quad \frac{I_3}{I_1} = 0.9343 \angle 142.96^\circ$$

These numerical results are in close agreement with Brown's [1804]. The dashed Hallén gains are not shown, as in the previous examples, because they are virtually indistinguishable from the sinusoidal ones (for  $M = 40$ ). □

**Example 25.5.4:** *Coupled Dolph-Chebyshev array.* In this example, we study the impact of mutual coupling on the array design methods of Chap. 23. For a typical array spacing of half-wavelength, the mutual impedance matrix is *diagonally dominant* and therefore, there will be some but minor impact on the design.

Fig. 25.5.7 shows a 15-element array of z-directed half-wavelength dipoles with spacing  $d = \lambda/2$  arranged along the x-axis. The antenna radii are  $a = 0.001\lambda$ .

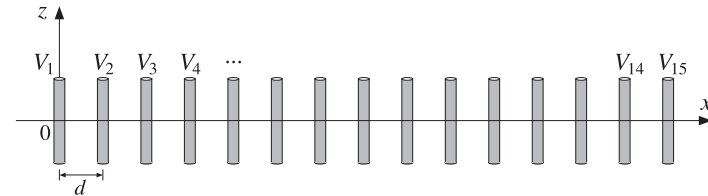


Fig. 25.5.7 Fifteen-element Dolph-Chebyshev array.

We take the feed voltages  $V = [V_1, V_2, \dots, V_{15}]^T$  to be Dolph-Chebyshev weights that would steer the azimuthal array gain towards  $\phi_0 = 120^\circ$  and would achieve a 20-dB side-lobe level. These weights can be designed with the function `dolph`.

If the mutual coupling is ignored, the impedance matrix  $Z$  will be proportional to the identity matrix because the antenna elements are identical. Then, the input currents  $I$  will be essentially equal to the driving voltages  $V$  and the array will behave according to the desired design.

If the mutual coupling is taken into account, the currents must be calculated from the solution of  $ZI = V$  and some distortions on the desired angular pattern may occur because  $Z$  is no longer diagonal.

Fig. 25.5.8 shows the azimuthal and polar gain patterns with and without mutual coupling. The primary effect is to distort the sidelobe levels so that they are no longer equal. But they are still acceptable as a close approximation to the desired Dolph-Chebyshev pattern.

The typical MATLAB code used in this example was as follows:

```
K = 15;
ph0 = 120; % steering angle

L = 0.5 * ones(1,K); % vector of antenna lengths
a = 0.001 * ones(1,K); % antenna radii
d = (0:K-1)*0.5; % equally-spaced with lambda/2 spacing

V = dolph(0.5, ph0, K, 20).'; % Dolph design with 20-dB sidelobes

Z = impedmat(L,a,d); % 15x15 impedance matrix
I = Z\V; % input currents

[ge,gh,ph] = gain2s(L,d,I,400,ph0); % gains with coupling

figure; dbz2(ph,gh); % azimuthal gain
figure; dbp2(ph,ge); % polar gain
```



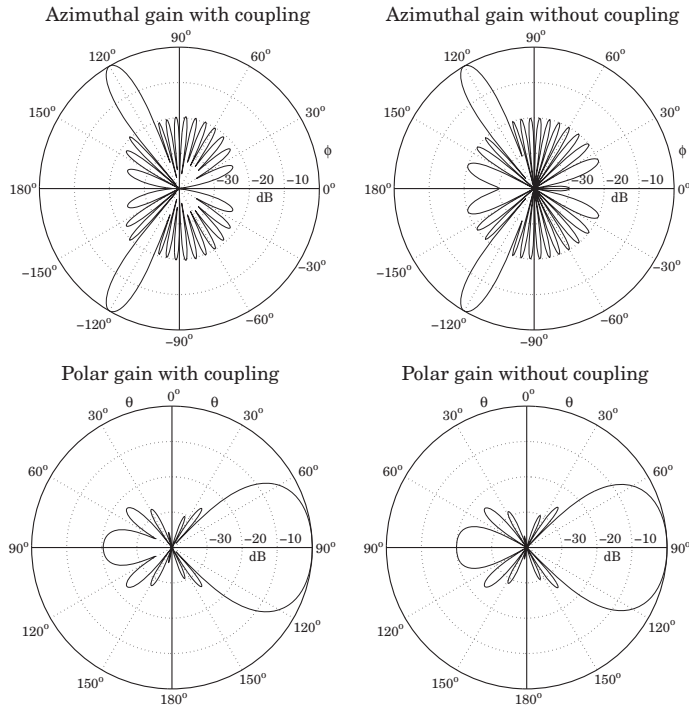


Fig. 25.5.8 H-plane and E-plane patterns with and without coupling.

```
[ge,gh,ph] = gain2s(L,d,V,400,ph0);           % gains without coupling
figure; dbz2(ph,gh);
figure; dbp2(ph,ge);
```

The E-plane polar gains were computed on the plane of the desired steering angle, that is,  $\phi_0 = 120^\circ$ . The figures show that maximum gain is at  $\theta = 90^\circ$  in the  $\phi_0$  direction. In the case without coupling, we set  $I = V$  inside gain2s because any proportionality constant gets canceled out. □

### 25.6 Yagi-Uda Antennas

A special type of parasitic array is the Yagi-Uda array shown in Fig. 25.6.1. The z-directed dipoles are arranged along the x-axis. The second dipole is driven; all others are parasitic.

The first dipole has length slightly longer than that of the driven dipole, and acts as a “reflector”. The elements to the right of the driven dipole have lengths slightly shorter,

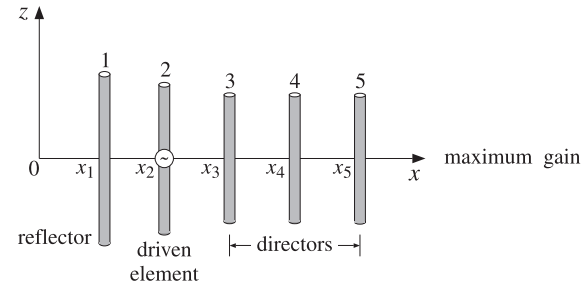


Fig. 25.6.1 Five-element Yagi-Uda array.

and act as “directors.” The reflector and directors direct the radiation preferentially towards endfire, that is, along the x-axis.

The Yagi-Uda array is widely used as a TV reception antenna and achieves fairly good directivity with such a simple structure. Good directivity characteristics are realized with certain choices for the antenna lengths and separations.

The analysis of the Yagi-Uda array follows the steps of the previous section. We assume that there are  $K$  dipoles, with the last  $K - 2$  being the directors, and that the currents are sinusoidal as in Eq. (25.4.16) because the antenna lengths are of the order of half-wavelength. Then, we compute the mutual impedance matrix  $Z$  and the input currents  $I = Z^{-1}V$ . Because only the second element is driven, the vector of voltages is:

$$V = [0, 1, \underbrace{0, 0, \dots, 0}_{(K-2) \text{ zeros}}]^T \tag{25.6.1}$$

Once we have the input currents  $I = [I_1, I_2, \dots, I_K]^T$ , the gain of the array is computed by Eq. (25.5.9), which simplifies into the following form because the dipoles lie along the x-axis:

$$g(\theta, \phi) = \left| \sum_{p=1}^K I_p \frac{\cos(kh_p \cos \theta) - \cos kh_p}{\sin kh_p \sin \theta} e^{j k x_p \sin \theta \cos \phi} \right|^2 \tag{25.6.2}$$

We assume that the lengths and separations are such that the maximum gain is towards endfire, that is, towards  $\theta = 90^\circ, \phi = 0^\circ$ . The forward and backward gains, and the *forward-backward* or *front-to-back* ratio are defined as:

$$g_f = g_{\max} = g(90^\circ, 0^\circ), \quad g_b = g(90^\circ, 180^\circ), \quad R_{fb} = \frac{g_f}{g_b} \tag{25.6.3}$$

It follows that the normalized gain will be  $g_n(\theta, \phi) = g(\theta, \phi)/g_f$ . Integrating it over all solid angles, we obtain the beam solid angle and hence the directivity of the Yagi-Uda array:

$$\Delta\Omega = \int_0^\pi \int_0^{2\pi} g_n(\theta, \phi) \sin \theta \, d\theta \, d\phi, \quad D = \frac{4\pi}{\Delta\Omega} \tag{25.6.4}$$

In dB, the directivity and forward-backward ratio are  $10\log_{10} D$  and  $10\log_{10} R_{fb}$ . The MATLAB function `yagi` implements the above design steps. It computes the input currents  $I$  as well as the directivity and forward-backward ratio. Its usage is:

```
[I,D,Rfb] = yagi(L,a,d); % Yagi-Uda array design
```

The function always assumes that the second element is the driven element and sets the value of  $V$  according to Eq. (25.6.1). The double integral in Eq. (25.6.4) is done with a 16-point Gauss-Legendre quadrature integration formula for each integration variable.

**Example 25.6.1: Reflectors and directors.** The simplest possible Yagi-Uda array has one driven element and either one reflector and no directors, or a single director and no reflector. Fig. 25.6.2 depicts the two cases.

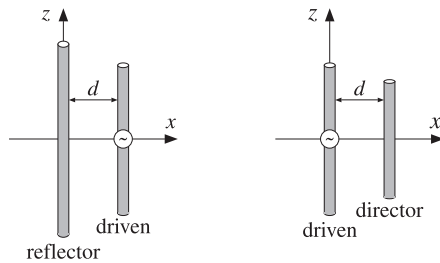


Fig. 25.6.2 The simplest Yagi-Uda arrays.

If the reflector is slightly longer than the driven element, and if the director is slightly shorter, then in both cases the radiation will be directed to the right, along the  $x$ -axis. Fig. 25.6.3 shows the resulting radiation patterns.

The length of the driven element was  $0.50\lambda$  and that of the reflector and director,  $0.54\lambda$  and  $0.46\lambda$ , respectively. The antenna radii were  $a = 0.003\lambda$  and their separation  $d = 0.1\lambda$ . The mutual impedances were calculated with `impedmat`:

$$Z = \begin{bmatrix} 92.47 + 104.19j & 75.68 + 11.63j \\ 75.68 + 11.63j & 73.07 + 41.37j \end{bmatrix}, \quad Z = \begin{bmatrix} 73.07 + 41.37j & 59.77 + 4.35j \\ 59.77 + 4.35j & 57.65 - 17.01j \end{bmatrix}$$

The typical MATLAB code that was used was:

```
L = [0.54, 0.50] % reflector case
a = 0.003*[1,1]; % radii
d = [0, 0.1]; % x-coordinates of locations

Z = impedmat(L,a,d); % impedance matrix
I = Z\ [0,1]'; % input currents

[ge,gh,th] = gain2s(L,d,I,400); % gain computation

figure; dbz2(th,gh,30,16); % azimuthal gain
figure; dbp2(th,ge,30,16); % polar gain
```

The driving voltages were in the two cases:  $V = [0, 1]^T$  and  $V = [1, 0]^T$ . □

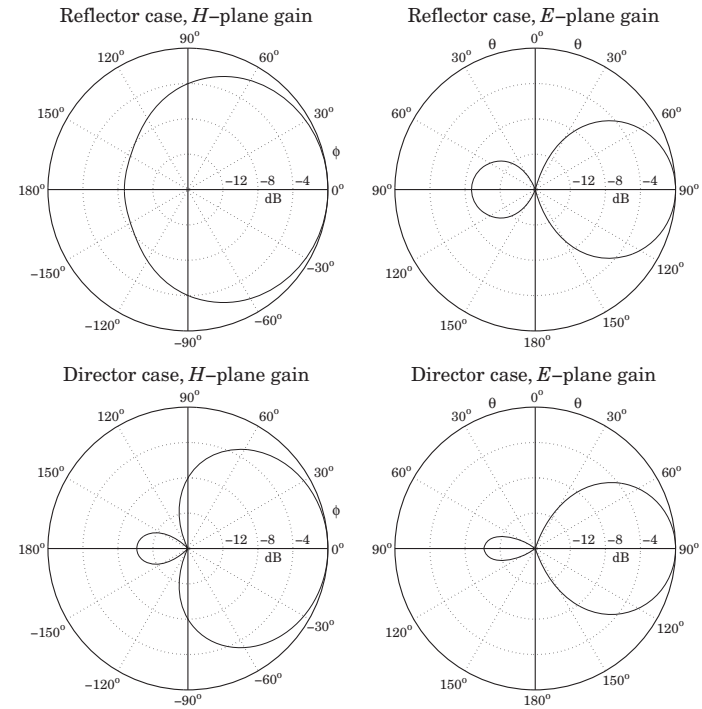


Fig. 25.6.3  $H$ -plane and  $E$ -plane gains of simple Yagi-Uda arrays.

**Example 25.6.2: Three-element Yagi.** Here, we consider a three-element Yagi-Uda array with one reflector, one driven element, and one director. The corresponding antenna lengths, radii, and locations along the  $x$ -axis (with the driven element at the origin) were in units of  $\lambda$ :

$$L = \begin{bmatrix} 0.50 \\ 0.48 \\ 0.46 \end{bmatrix}, \quad \mathbf{a} = \begin{bmatrix} 0.003 \\ 0.003 \\ 0.003 \end{bmatrix}, \quad \mathbf{d} = \begin{bmatrix} x_1 \\ x_2 \\ x_3 \end{bmatrix} = \begin{bmatrix} -0.125 \\ 0 \\ 0.125 \end{bmatrix}$$

The azimuthal and polar gains are shown in Fig. 25.6.4. The dashed gains correspond to the exact coupled Hallén equations, as discussed in Example 25.7.3. The computed directivity and front/back ratio were  $D = 8.18$  dB and  $R_{fb} = 18.69$  dB. Thus, the array achieves a gain of  $D - 2.15 = 6.03$  dB over a single half-wavelength dipole.

The impedance matrix was:

$$Z = \begin{bmatrix} 73.07 + 41.37j & 60.47 - 0.97j & 36.25 - 25.53j \\ 60.47 - 0.97j & 64.93 + 11.75j & 53.72 - 2.71j \\ 36.25 - 25.53j & 53.72 - 2.71j & 57.65 - 17.01j \end{bmatrix}$$

The input currents and input impedance of the driving element were:

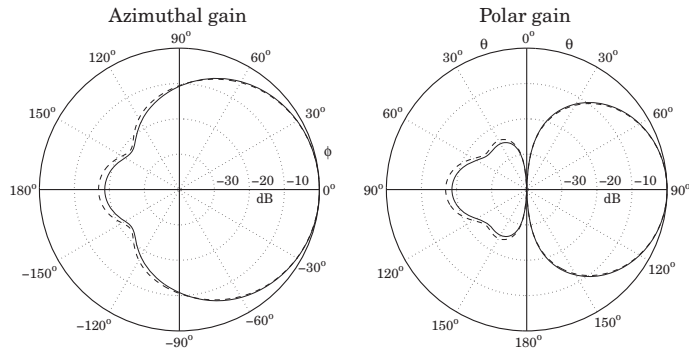


Fig. 25.6.4 Azimuthal and polar gains of three-element Yagi-Uda array.

$$I = \begin{bmatrix} I_1 \\ I_2 \\ I_3 \end{bmatrix} = \begin{bmatrix} -0.0290 + 0.0176j \\ 0.1062 - 0.0182j \\ -0.0801 - 0.0256j \end{bmatrix}, \quad Z_2 = \frac{V_2}{I_2} = \frac{1}{I_2} = 9.15 + 1.57j$$

The typical MATLAB code for this example was:

```
L = [0.50, 0.48, 0.46];           % antenna lengths
a = 0.003*[1,1,1];               % radii
d = [-0.125, 0, 0.125];         % x-locations

[I,D,Rfb] = yagi(L,a,d);         % solve ZI = V

[ge,gh,th] = gain2s(L,d,I,360); % compute gains at 1° increments

M = 40;                           % number of upper-half samples

[I,z] = hcoupled(L,a,d,[0,1,0],M); % compute Hallén currents

[ge2,gh2,ph] = gain2d(L,d,I,360); % gain of Hallén currents

figure; dbz2(ph,gh); dbadd2(2,'--',ph,gh2);
figure; dbp2(ph,ge); dbadd2(1,'--',ph,ge2);
```

The driving voltages were defined within `yagi` to be  $V = [0, 1, 0]^T$ . □

**Example 25.6.3:** *Optimized six-element Yagi.* Chen and Cheng [1818] applied King's three-term current approximation [4] and devised procedures for optimizing the choices of the antenna lengths and separations of Yagi-Uda arrays. Fig. 25.6.5 shows the gains before and after optimization of a six-element Yagi-Uda array calculated with the functions `yagi` and `gain2s`. The antenna radii were  $a = 0.003369\lambda$ .

For the unoptimized case, the antenna lengths and  $x$ -locations were in units of  $\lambda$ :

$$L = [L_1, L_2, L_3, L_4, L_5, L_6] = [0.510, 0.490, 0.430, 0.430, 0.430, 0.430]$$

$$d = [x_1, x_2, x_3, x_4, x_5, x_6] = [-0.25, 0, 0.310, 0.620, 0.930, 1.240]$$

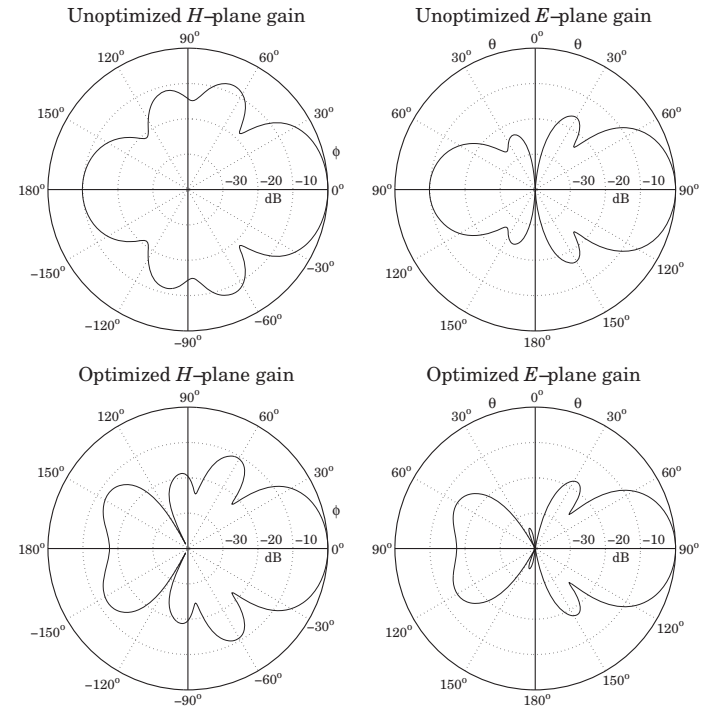


Fig. 25.6.5 Gains of six-element Yagi-Uda array.

The directors were identical and equally spaced at spacing of  $0.31\lambda$ . The computed directivity and front/back ratio were 11 dB and 9.84 dB, respectively. The optimized case has slightly different lengths and  $x$ -locations:

$$L = [L_1, L_2, L_3, L_4, L_5, L_6] = [0.476, 0.452, 0.436, 0.430, 0.434, 0.430]$$

$$d = [x_1, x_2, x_3, x_4, x_5, x_6] = [-0.25, 0, 0.289, 0.695, 1.018, 1.440]$$

Typical MATLAB code was as follows:

```
L = [0.476, 0.452, 0.436, 0.430, 0.434, 0.430];
a = 0.003369 * [1,1,1,1,1,1];
d = [-0.25, 0, 0.289, 0.695, 1.018, 1.440];

[I,D,Rfb] = yagi(L,a,d);

[ge,gh,th] = gain2s(L,d,I,360);

figure; dbz2(th,gh,30,40);
figure; dbp2(th,ge,30,40);
```

The optimized directivity was 12.54 dB and the forward/backward ratio 17.6 dB. □

### 25.7 Hallén Equations for Coupled Antennas

In Sects. 25.4 and 25.5, we developed the Hallén-Pocklington equations for coupled antennas, that is, Eqs. (25.4.8)-(25.4.9) and (25.5.1). Here, we discuss their numerical solution. On the  $p$ th antenna, we have:

$$(\partial_z^2 + k^2)V_p(z) = 2kV_p\delta(z), \quad p = 1, 2, \dots, K \quad (25.7.1)$$

where  $V_p$  is the driving delta-gap input and  $V_p(z)$  is the sum of the (scaled) vector potentials due to the currents on all antennas:

$$V_p(z) = \sum_{q=0}^K V_{pq}(z) = \frac{j\eta}{2\pi} \sum_{q=0}^K \int_{-h_q}^{h_q} G_{pq}(z-z') I_q(z') dz' \quad (25.7.2)$$

where we recall the definition of the impedance kernel:

$$G_{pq}(z-z') = \frac{e^{-jkR}}{R}, \quad R = \sqrt{(z-z')^2 + d_{pq}^2} \quad (25.7.3)$$

and  $d_{pq}$  are the mutual distances or radii, as defined in Eq. (25.5.2). The use of the approximate kernel in (25.7.3) is well-justified for the off-diagonal terms ( $p \neq q$ ) because the distances  $d_{pq}$  are typically much greater than the radii. However, for the diagonal term ( $p = q$ ), one could use the exact kernel given as in (24.7.10) by,

$$G_{pp}(z-z') = \frac{2}{\pi} \int_0^{\pi/2} \frac{e^{-jkR}}{R} d\theta, \quad R = \sqrt{(z-z')^2 + 4a_p^2 - 4a_p^2 \sin^2 \theta} \quad (25.7.4)$$

Following the discussion of Sec. 24.3, the solution of (25.7.1) is of the form:

$$V_p(z) = C_p \cos kz + V_p \sin k|z|, \quad -h_p \leq z \leq h_p \quad (25.7.5)$$

where we assumed that all the antennas are center-driven, and therefore,  $V_p(z)$  will be even in  $z$ . Combining (25.7.5) with (25.7.2), we obtain the *coupled system of Hallén equations*, for  $p = 1, 2, \dots, K$ :

$$\frac{j\eta}{2\pi} \sum_{q=0}^K \int_{-h_q}^{h_q} G_{pq}(z-z') I_q(z') dz' = C_p \cos kz + V_p \sin k|z| \quad (25.7.6)$$

The  $K$  constants  $C_1, C_2, \dots, C_K$  are determined by imposing the end conditions on the  $K$  currents:  $I_p(h_p) = 0$ , for  $p = 1, 2, \dots, K$ .

To solve this system, we use a basis-function expansion of the form of Eq. (24.8.3) and apply point matching. For simplicity, we take the same number of sampling points on each antenna,  $N = 2M + 1$ . Because the antenna lengths may be different, the sample spacings will also be different. On the  $q$ th antenna we have,

$$z_m = m\Delta_q, \quad \Delta_q = \frac{2h_q}{2M+1} = \frac{l_q}{N}, \quad -M \leq m \leq M \quad (25.7.7)$$

The basis-function expansion for the  $q$ th current is

$$I_q(z') = \sum_{m=-M}^M I_q(z_m) B_q(z' - z_m), \quad q = 1, 2, \dots, K \quad (25.7.8)$$

We are going to use only the pulse and the triangular bases defined by Eqs. (24.8.4) and (24.11.2), respectively, with sample spacing  $\Delta = \Delta_q$ . For the triangular basis, we must set  $\Delta_q = h_q/M$  instead of  $\Delta_q = 2h_q/(2M+1)$ .

Inserting (25.7.8) into (25.7.6) and sampling along the  $p$ -th antenna, that is, at the points  $z_n = n\Delta_p$ , for  $-M \leq n \leq M$ , we obtain the discretized system:

$$\frac{j\eta}{2\pi} \sum_{q=0}^K \sum_{m=-M}^M I_q(z_m) \int_{-h_q}^{h_q} G_{pq}(z_n - z') B_q(z' - z_m) dz' = C_p \cos kz_n + V_p \sin k|z_n|$$

We define the  $N \times N$  impedance matrix  $Z_{pq}$  whose  $nm$ th matrix element is:

$$\begin{aligned} Z_{pq}(n, m) &= \frac{j\eta}{2\pi} \int_{-h_q}^{h_q} G_{pq}(z_n - z') B_q(z' - z_m) dz' \\ &= \frac{j\eta}{2\pi} \int_{-h_q}^{h_q} G_{pq}(z_n - z_m - z) B_q(z) dz \end{aligned} \quad (25.7.9)$$

with  $-M \leq n, m \leq M$ . In particular, for the pulse basis, these take the form:

$$Z_{pq}(n, m) = \frac{j\eta}{2\pi} \int_{-\Delta_q/2}^{\Delta_q/2} G_{pq}(z_n - z_m - z) dz \quad (25.7.10)$$

and, for the triangular basis:

$$Z_{pq}(n, m) = \frac{j\eta}{2\pi} \int_{-\Delta_q}^{\Delta_q} \left(1 - \frac{|z|}{\Delta_q}\right) G_{pq}(z_n - z_m - z) dz \quad (25.7.11)$$

Denoting  $I_q(m) = I_q(z_m)$ , the discretized Hallén system becomes:

$$\sum_{q=0}^K \sum_{m=-M}^M Z_{pq}(n, m) I_q(m) = C_p \cos kz_n + V_p \sin k|z_n| \quad (25.7.12)$$

where  $p = 1, 2, \dots, K$ . And, written in a more compact form:

$$\sum_{q=0}^K Z_{pq} \mathbf{I}_q = C_p \mathbf{c}_p + V_p \mathbf{s}_p \quad (25.7.13)$$

where we defined the  $N$ -dimensional vectors:

$$\mathbf{I}_q = \begin{bmatrix} I_q(M) \\ \vdots \\ I_q(1) \\ I_q(0) \\ I_q(1) \\ \vdots \\ I_q(M) \end{bmatrix}, \quad \mathbf{c}_p = \begin{bmatrix} \cos kz_M \\ \vdots \\ \cos kz_1 \\ \cos kz_0 \\ \cos kz_1 \\ \vdots \\ \cos kz_M \end{bmatrix}, \quad \mathbf{s}_p = \begin{bmatrix} \sin kz_M \\ \vdots \\ \sin kz_1 \\ \sin kz_0 \\ \sin kz_1 \\ \vdots \\ \sin kz_M \end{bmatrix} \quad (25.7.14)$$

and used the even symmetry in  $z$ . The vectors  $\mathbf{c}_p$  and  $\mathbf{s}_p$  depend on  $p$  through the sample spacing in  $z_n = n\Delta_p, -M \leq n \leq M$ .

The system (25.7.13) provides  $K$  coupled matrix equations by which to determine the  $K$  sampled current vectors  $\mathbf{I}_1, \mathbf{I}_2, \dots, \mathbf{I}_K$  on each antenna. The  $N \times N$  matrices  $Z_{pq}$  are not Toeplitz, unless the antennas are identical, in which case  $\Delta_p = \Delta_q$  and the  $Z_{pq}(n, m)$  depends only on the difference  $n - m$ . Of course, for  $p = q$ ,  $Z_{pp}$  is both symmetric and Toeplitz.

However, while not Toeplitz, the matrix  $Z_{pq}$  is reversal-invariant because of the property  $Z_{pq}(n, m) = Z_{pq}(-n, -m)$ , which follows from Eq. (25.7.9). Therefore, the matrix system (25.7.13) can be wrapped in half by the procedure discussed in Sec. 24.9, which replaced the matrix equation (24.9.6) by (24.9.7).

Here, each  $N \times N$  matrix  $Z_{pq}$  is wrapped to size  $(M + 1) \times (M + 1)$  by the same process. The resulting system looks identical to (25.7.13), except the currents and right-hand sides are essentially half those of (25.7.14):

$$\mathbf{I}_q = \begin{bmatrix} I_q(0) \\ I_q(1) \\ \vdots \\ I_q(M) \end{bmatrix}, \quad \mathbf{c}_p = \begin{bmatrix} \cos kZ_0 \\ \cos kZ_1 \\ \vdots \\ \cos kZ_M \end{bmatrix}, \quad \mathbf{s}_p = \begin{bmatrix} \sin kZ_0 \\ \sin kZ_1 \\ \vdots \\ \sin kZ_M \end{bmatrix} \quad (25.7.15)$$

In particular, if all antennas are identical, then the wrapping process can be made even more efficient using the Toeplitz-Hankel properties of the wrapped matrices, as discussed in Example 24.9.1. In any case, we will assume in the sequel that the system (25.7.13) has been wrapped in half.

If the constants  $C_p$  were known, the solution of the system (25.7.13) could be obtained by writing it as a *single block-matrix* linear system of the form:

$$\boxed{\mathbf{Z}\mathbf{I} = \mathbf{C}\mathbf{c} + \mathbf{V}\mathbf{s}} \quad (25.7.16)$$

where  $\mathbf{Z}$  is the  $K \times K$  block matrix whose  $pq$ th matrix element is the  $(M + 1) \times (M + 1)$  matrix  $Z_{pq}$ , and  $\mathbf{C}, \mathbf{V}$  are appropriate block-diagonal matrices. The vectors  $\mathbf{I}, \mathbf{c}, \mathbf{s}$  are the concatenations of  $\mathbf{I}_p, \mathbf{c}_p, \mathbf{s}_p$ . For example, in the case  $K = 3$ , the system (25.7.13) reads:

$$\begin{aligned} Z_{11}\mathbf{I}_1 + Z_{12}\mathbf{I}_2 + Z_{13}\mathbf{I}_3 &= C_1\mathbf{c}_1 + V_1\mathbf{s}_1 \\ Z_{21}\mathbf{I}_1 + Z_{22}\mathbf{I}_2 + Z_{23}\mathbf{I}_3 &= C_2\mathbf{c}_2 + V_2\mathbf{s}_2 \\ Z_{31}\mathbf{I}_1 + Z_{32}\mathbf{I}_2 + Z_{33}\mathbf{I}_3 &= C_3\mathbf{c}_3 + V_3\mathbf{s}_3 \end{aligned}$$

This can be written in the  $3 \times 3$  block-matrix form:

$$\begin{bmatrix} Z_{11} & Z_{12} & Z_{13} \\ Z_{21} & Z_{22} & Z_{23} \\ Z_{31} & Z_{32} & Z_{33} \end{bmatrix} \begin{bmatrix} \mathbf{I}_1 \\ \mathbf{I}_2 \\ \mathbf{I}_3 \end{bmatrix} = \begin{bmatrix} C_1I & 0 & 0 \\ 0 & C_2I & 0 \\ 0 & 0 & C_3I \end{bmatrix} \begin{bmatrix} \mathbf{c}_1 \\ \mathbf{c}_2 \\ \mathbf{c}_3 \end{bmatrix} + \begin{bmatrix} V_1I & 0 & 0 \\ 0 & V_2I & 0 \\ 0 & 0 & V_3I \end{bmatrix} \begin{bmatrix} \mathbf{s}_1 \\ \mathbf{s}_2 \\ \mathbf{s}_3 \end{bmatrix}$$

where  $I$  is the  $(M + 1) \times (M + 1)$  identity matrix.

Next, we discuss the determination of the constants  $C_p$ . The condition  $I_p(M) = 0$  can be written vectorially in the form  $\mathbf{u}^T \mathbf{I}_p = 0$ , where  $\mathbf{u} = [0, \dots, 0, 1]^T$ , as was done in Sec. 24.9. Separating the  $p$ th term of the  $p$ th equation in (25.7.13), we have:

$$Z_{pp}\mathbf{I}_p + \sum_{q \neq p} Z_{pq}\mathbf{I}_q = C_p\mathbf{c}_p + V_p\mathbf{s}_p \quad (25.7.17)$$

Solving for  $\mathbf{I}_p$  and multiplying by  $\mathbf{u}^T$ , we obtain the condition:

$$\mathbf{u}^T \mathbf{I}_p = C_p \mathbf{u}^T Z_{pp}^{-1} \mathbf{c}_p + V_p \mathbf{u}^T Z_{pp}^{-1} \mathbf{s}_p - \sum_{q \neq p} \mathbf{u}^T Z_{pp}^{-1} Z_{pq} \mathbf{I}_q = 0$$

Defining the quantity  $\mathbf{u}_p = Z_{pp}^{-1} \mathbf{u}$ , we solve this condition for  $C_p$ :

$$C_p = \frac{1}{\mathbf{u}_p^T \mathbf{c}_p} \left( \sum_{q \neq p} \mathbf{u}_p^T Z_{pq} \mathbf{I}_q - V_p \mathbf{u}_p^T \mathbf{s}_p \right)$$

Inserting  $C_p$  into Eq. (25.7.17) and rearranging terms, we obtain:

$$Z_{pp}\mathbf{I}_p + \sum_{q \neq p} \left( I - \frac{\mathbf{c}_p \mathbf{u}_p^T}{\mathbf{c}_p^T \mathbf{u}_p} \right) Z_{pq} \mathbf{I}_q = V_p \left( I - \frac{\mathbf{c}_p \mathbf{u}_p^T}{\mathbf{c}_p^T \mathbf{u}_p} \right) \mathbf{s}_p \quad (25.7.18)$$

To simplify it, we define the  $(M + 1) \times (M + 1)$  *projection* matrices:

$$\mathcal{P}_p = I - \frac{\mathbf{c}_p \mathbf{u}_p^T}{\mathbf{c}_p^T \mathbf{u}_p}, \quad p = 1, 2, \dots, K \quad (25.7.19)$$

Then, Eq. (25.7.18) can be written in the form:

$$\tilde{Z}_{pp}\mathbf{I}_p + \sum_{q \neq p} \mathcal{P}_p Z_{pq} \mathbf{I}_q = V_p \mathcal{P}_p \mathbf{s}_p \quad (25.7.20)$$

Thus, eliminating the constants  $C_p$  by enforcing the end conditions, amounts to replacing the impedance matrices  $Z_{pq}$  by the projected ones:

$$\tilde{Z}_{pq} = \begin{cases} Z_{pp}, & \text{if } q = p \\ \mathcal{P}_p Z_{pq}, & \text{if } q \neq p \end{cases} \quad (25.7.21)$$

and the term  $\mathbf{s}_p$  by the projected one,  $\tilde{\mathbf{s}}_p = \mathcal{P}_p \mathbf{s}_p$ . Then, Eq. (25.7.20) can be written in the form:

$$\boxed{\sum_{q=0}^K \tilde{Z}_{pq} \mathbf{I}_q = V_p \tilde{\mathbf{s}}_p}, \quad p = 1, 2, \dots, K \quad (25.7.22)$$

or, compactly in the block-matrix form:

$$\boxed{\tilde{\mathbf{Z}}\mathbf{I} = \mathbf{V}\tilde{\mathbf{s}}} \quad (25.7.23)$$

with solution:

$$\mathbf{I} = \begin{bmatrix} \mathbf{I}_1 \\ \mathbf{I}_2 \\ \vdots \\ \mathbf{I}_K \end{bmatrix} = \tilde{\mathbf{Z}}^{-1} \mathbf{V}\tilde{\mathbf{s}} = \tilde{\mathbf{Z}}^{-1} \begin{bmatrix} V_1 \tilde{\mathbf{s}}_1 \\ V_2 \tilde{\mathbf{s}}_2 \\ \vdots \\ V_K \tilde{\mathbf{s}}_K \end{bmatrix} \quad (25.7.24)$$

The MATLAB function `hcoupled` implements the above solution procedure. First, it constructs the impedance matrices  $Z_{pq}$  by calculating the integrals in Eq. (25.7.9) using a 32-point Gauss-Legendre quadrature integration formula. Second, it wraps the matrices  $Z_{pq}$  in half and puts them together into the block-matrix  $\tilde{\mathbf{Z}}$ . And third, it constructs the projected matrix  $\tilde{\mathbf{Z}}$  and the solution (25.7.24). Its usage is:

```
[I, z] = hcoupled(L, a, d, V, M, ker, basis); % solve Hallén equations for coupled dipoles
```

where  $L, a, d$  are the vectors of antenna lengths, radii, and  $xy$ -locations, and  $V$  is the vector of the driving voltages  $V = [V_1, V_2, \dots, V_K]$ . The parameters  $L, a, d$  have the same usage as in the functions `yagi` and `gain2s`. The string input `ker` takes the values 'e', 'a' for using the exact or the approximate kernel in the computation of the diagonal elements of the impedance matrix. The `basis` parameter can take only the two values 'p', 't' for pulse or triangular basis.

The output  $I$  is the  $(2M + 1) \times K$  matrix whose  $p$ th column is the double-sided vector of current samples  $I_p(z_m)$ ,  $z_m = m\Delta_p$ ,  $-M \leq m \leq M$ . Thus, the matrix elements of  $I$  are  $I(m, p) = I_p(z_m)$ . Similarly, the  $p$ th column of the output matrix  $z$  holds the sampled  $z$ -locations on the  $p$ th antenna, that is,  $z(m, p) = m\Delta_p$ .

The output matrix  $I$  is obtained by using the MATLAB function `reshape` to reshape the  $(K(M + 1))$ -dimensional column vector solution (25.7.24) into a matrix of size  $(M + 1) \times K$ , and then, symmetrizing it to size  $(2M + 1) \times K$ .

A faster version of `hcoupled` is the function `hcoupled2`, which assumes that the antennas are identical. It is faster because it makes use of the Toeplitz-Hankel structure of the wrapped matrices  $Z_{pq}$  to construct them more efficiently. Its usage is:

```
[I, z] = hcoupled2(L, a, d, V, M, ker, basis); % Hallén equations for coupled identical dipoles
```

where  $I$  has the same meaning as in `hcoupled`, but  $z$  is now a single column vector, that is,  $z_m = m\Delta$ ,  $-M \leq m \leq M$ . In both `hcoupled2` and `hcoupled`, the final solution is obtained by solving the system (25.7.23), which is  $(K(M + 1)) \times (K(M + 1))$ -dimensional.

In order to conveniently manipulate the block impedance matrices, we developed a MATLAB function, `blockmat`, which is used extensively inside `hcoupled2` and `hcoupled`. It allows one to create block matrices and to extract or insert sub-blocks. Its usage is as follows:

```
Z = blockmat(K, K, M+1, M+1); % create a (K(M + 1)) x (K(M + 1)) matrix of zeros
Zpq = blockmat(K, K, p, q, Z); % extract pqth submatrix of Z
Z = blockmat(K, K, p, q, Z, Zpq); % insert Zpq into pqth submatrix of Z
s = blockmat(K, 1, M+1, 1); % create a (K(M + 1))-dimensional column of zeros
sp = blockmat(K, 1, p, 1, s); % extract the pth subvector of s
s = blockmat(K, 1, p, 1, s, sp); % insert sp into pth subvector of s
```

Once the sampled currents  $I_p(m)$  are known, the gain of the array can be computed by finding the total current density,  $J(\mathbf{r}) = \hat{z}J_z(\mathbf{r})$ :

$$J_z(\mathbf{r}) = \sum_{p=1}^K I_p(z) \delta(x - x_p) \delta(y - y_p) = \sum_{p=1}^K \sum_{m=-M}^M I_p(m) B_p(z - z_m) \delta(x - x_p) \delta(y - y_p)$$

where we used Eq. (25.7.8). The corresponding radiation vector is:

$$F_z(\theta, \phi) = \int J_z(\mathbf{r}) e^{jk \cdot \mathbf{r}} d^3 \mathbf{r} = \sum_{m=-M}^M \sum_{p=1}^K I_p(m) e^{jk_x x_p + jk_y y_p} \int_{-h_p}^{h_p} B_p(z - z_m) e^{jk_z z} dz$$

$$= \sum_{m=-M}^M \sum_{p=1}^K I_p(m) e^{jk_x x_p + jk_y y_p} e^{jk_z z_m} \int_{-h_p}^{h_p} B_p(z) e^{jk_z z} dz$$

Performing the  $z$ -integration, we finally get:

$$F_z(\theta, \phi) = \sum_{m=-M}^M \sum_{p=1}^K I_p(m) e^{jk_x x_p + jk_y y_p} \Delta_p \left[ \frac{\sin(k_z \Delta_p / 2)}{k_z \Delta_p / 2} \right]^b \quad (25.7.25)$$

where  $k_x = k \sin \theta \cos \phi$ ,  $k_y = k \sin \theta \sin \phi$ , and  $k_z = k \cos \theta$ , and  $b = 1$  for the pulse basis and  $b = 2$  for the triangular one. The corresponding normalized gain of the array will be, up to a constant:

$$g(\theta, \phi) = |\sin \theta F_z(\theta, \phi)|^2 \quad (25.7.26)$$

The MATLAB function `gain2d` computes the  $E$ -plane polar gain and the  $H$ -plane azimuthal gain from Eqs. (25.7.25) and (25.7.26). Its usage is:

```
[ge, gh, th] = gain2d(L, d, I, N, ph0, basis) % gain of 2D array of antennas with Hallén currents
[ge, gh, th] = gain2d(L, d, I, N, ph0) % equivalent to basis='p' (pulse basis)
[ge, gh, th] = gain2d(L, d, I, N, basis) % equivalent to ph0=0
[ge, gh, th] = gain2d(L, d, I, N) % equivalent to ph0=0, basis='p'
```

where the current input  $I$  is exactly the same as the output matrix from `hcoupled` or `hcoupled2`. The meaning of the outputs are exactly the same as in the function `gain2s` discussed in Sec. 25.5. The string `basis` takes the values 'p' or 't', for pulse or triangular basis.

The difference between `gain2s` and `gain2d` is that the former assumes the currents are sinusoidal and  $I$  represents only the input currents,  $I = [I_1, I_2, \dots, I_K]$ . whereas in the latter, the full  $(2M + 1) \times K$  current matrix is needed,  $I = [I_1, I_2, \dots, I_K]$ .

**Example 25.7.1:** *Hallén solution of parasitic array.* Consider the three-element array of Example 25.5.1 and shown in Fig. 25.5.2. The Hallén currents on each antenna can be computed by using `hcoupled2` because the elements are identical. Fig. 25.7.1 shows the computed sampled currents with  $N = 2M + 1 = 81$  or  $M = 40$ .

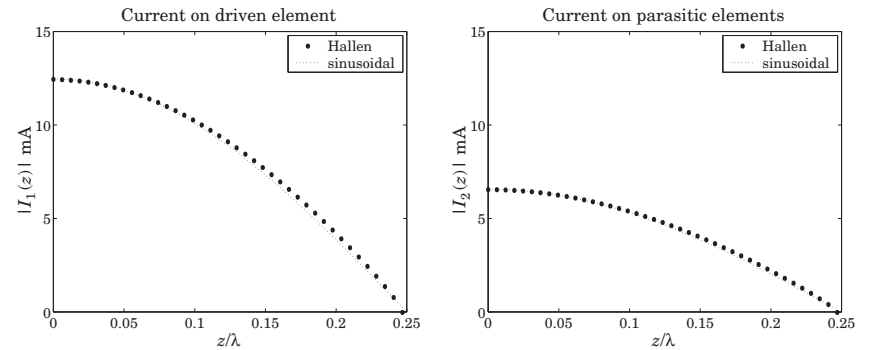


Fig. 25.7.1 Currents on driven and parasitic antennas.

Because of the symmetry, the currents on the two parasitic antennas are the same. For all three antennas, the currents are essentially sinusoidal, justifying the use of this assumption. The gains computed with `gain2d`, and under the sinusoidal assumption with `gain2s`,



were shown in Fig. 25.5.3. The MATLAB code used to generate the currents and the gains was given in Example 25.5.1. □

**Example 25.7.2:** *Full-wavelength parasitic array.* If one or more of the antennas has length equal to a multiple of  $\lambda$ , the analysis methods based on the sinusoidal assumption break down because the impedance matrix computed with Eq. (25.4.15) becomes infinite.

On the other hand, the numerical solution of the Hallén system can still be carried through giving a finite answer. Fig. 25.7.2 shows the gains and currents of the parasitic array of Example 25.5.1, but all the antennas being full-wavelength elements,  $l = \lambda$ . The distance of the parasitic antennas to the driven element was also changed to  $d = 0.25\lambda$  from  $d = 0.5\lambda$ .

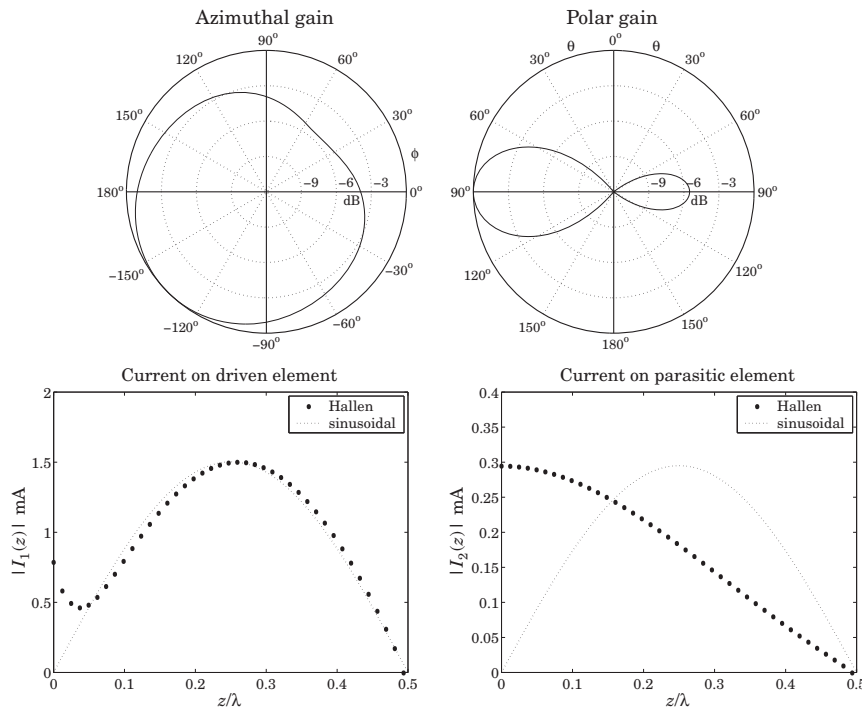


Fig. 25.7.2 Gains and currents of full-wavelength parasitic array.

The sinusoidal assumption for the driven element is fairly accurate except near  $z = 0$ , where the current has a non-zero value. But on the parasitic element, the sinusoidal assumption is completely wrong. □

**Example 25.7.3:** *Three-element Yagi-Uda array.* Here, we compute the currents on the three antennas of the Yagi-Uda array of Example 25.6.2. Because the antennas are not identical, the function `hcoupled` must be used. The gains were computed with `gain2s` and `gain2d` in Example 25.6.2, and shown in Fig. 25.6.4. The sampled currents on the three antennas are shown in Fig. 25.7.3.

We observe that the sinusoidal assumption is fairly accurate. The MATLAB code used to generate the current graphs was as follows:

```
L = [0.50, 0.48, 0.46]; h = L/2;
a = 0.003 * [1, 1, 1];
d = [-0.125, 0, 0.125];
V = [0, 1, 0]; % can be defined as column or row

k = 2*pi;
M = 40;

[I, z] = hcoupled(L, a, d, V, M);

I1 = abs(I(M+1:end, 1)); m1 = max(I1); z1 = z(M+1:end, 1);
I2 = abs(I(M+1:end, 2)); m2 = max(I2); z2 = z(M+1:end, 2);
I3 = abs(I(M+1:end, 3)); m3 = max(I3); z3 = z(M+1:end, 3);

s1 = 0:h(1)/50:h(1); Is1 = m1*abs(sin(k*(h(1)-s1)));
s2 = 0:h(2)/50:h(2); Is2 = m2*abs(sin(k*(h(2)-s2)));
s3 = 0:h(3)/50:h(3); Is3 = m3*abs(sin(k*(h(3)-s3)));

figure; plot(z1, I1, '.', s1, Is1, ':');
figure; plot(z2, I2, '.', s2, Is2, ':');
figure; plot(z3, I3, '.', s3, Is3, ':');
```

Note that  $I_1$ ,  $I_2$ , and  $I_3$  are obtained from the three columns of  $I$ , and  $z_1$ ,  $z_2$ , and  $z_3$  from the three columns of  $z$ . Only the currents on the upper-half of each antenna are plotted. The sinusoidal currents are scaled to the maximum values of the corresponding Hallén currents.

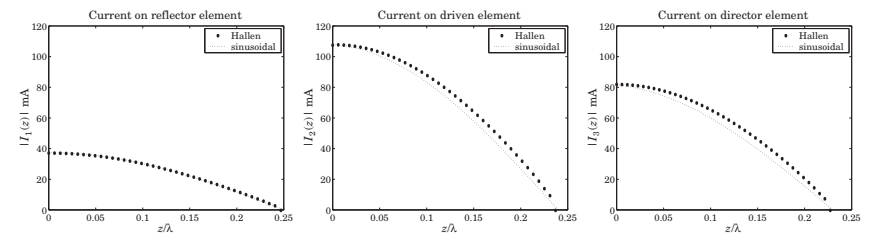


Fig. 25.7.3 Currents on the Yagi antennas.

These examples demonstrate the remark made earlier that the sinusoidal assumption is justified only for antennas with lengths near half a wavelength. □

### 25.8 Problems

25.1 Show that the asymptotic form of Eq. (25.3.7) for the mutual impedance between two parallel dipoles separated by a distance  $d$  is given by

$$Z_{21} = \frac{j\eta}{\pi} \tan\left(\frac{kh_1}{2}\right) \tan\left(\frac{kh_2}{2}\right) \frac{e^{-jkd}}{kd}, \text{ for large } d$$



25.2 Using the higher-order terms in the series (25.3.23), show that the input impedance  $Z_{\text{in}} = R + jX$  of a small dipole is given as follows to order  $(kl)^4$ , where  $L = \ln(2a/l)$ :

$$R = \frac{\eta}{2\pi} \left[ \frac{1}{12} (kl)^2 + \frac{1}{360} (kl)^4 \right], \quad X = \frac{\eta}{2\pi} \left[ \frac{4(1+L)}{kl} - \frac{1}{3} \left( L + \frac{2}{3} \right) (kl) - \frac{1}{180} \left( L - \frac{11}{30} \right) (kl)^3 \right]$$

25.3 Consider a small dipole with a linear current given by Eq. (25.3.25). Determine the radiation vector, and the radiated electric and magnetic fields at a far distance  $r$  from the dipole. Calculate the radiated power  $P_{\text{rad}}$  by integrating the radial Poynting vector over a large sphere. Then identify the radiation resistance  $R$  through the definition:

$$P_{\text{rad}} = \frac{1}{2} R |I_0|^2$$

and show  $R$  is the same as that given by Eq. (25.3.24)

### A. Physical Constants

We use SI units throughout this text. Simple ways to convert between SI and other popular units, such as Gaussian, may be found in Refs. [123–126].

The Committee on Data for Science and Technology (CODATA) of NIST maintains the values of many physical constants [112]. The most current values can be obtained from the CODATA web site [1823]. Some commonly used constants are listed below:

quantity	symbol	value	units
speed of light in vacuum	$c_0, c$	299 792 458	$\text{m s}^{-1}$
permittivity of vacuum	$\epsilon_0$	$8.854\,187\,817 \times 10^{-12}$	$\text{F m}^{-1}$
permeability of vacuum	$\mu_0$	$4\pi \times 10^{-7}$	$\text{H m}^{-1}$
characteristic impedance	$\eta_0, Z_0$	376.730 313 461	$\Omega$
electron charge	$e$	$1.602\,176\,462 \times 10^{-19}$	C
electron mass	$m_e$	$9.109\,381\,887 \times 10^{-31}$	kg
Boltzmann constant	$k$	$1.380\,650\,324 \times 10^{-23}$	$\text{JK}^{-1}$
Avogadro constant	$N_A, L$	$6.022\,141\,994 \times 10^{23}$	$\text{mol}^{-1}$
Planck constant	$h$	$6.626\,068\,76 \times 10^{-34}$	J/Hz
Gravitational constant	$G$	$6.672\,59 \times 10^{-11}$	$\text{m}^3 \text{kg}^{-1} \text{s}^{-2}$
Earth mass	$M_\oplus$	$5.972 \times 10^{24}$	kg
Earth equatorial radius	$a_e$	6378	km

In the table, the constants  $c, \mu_0$  are taken to be exact, whereas  $\epsilon_0, \eta_0$  are derived from the relationships:

$$\epsilon_0 = \frac{1}{\mu_0 c^2}, \quad \eta_0 = \sqrt{\frac{\mu_0}{\epsilon_0}} = \mu_0 c$$

The energy unit of electron volt (eV) is defined to be the work done by an electron in moving across a voltage of one volt, that is,  $1 \text{ eV} = 1.602\,176\,462 \times 10^{-19} \text{ C} \cdot 1 \text{ V}$ , or

$$1 \text{ eV} = 1.602\,176\,462 \times 10^{-19} \text{ J}$$